Lipidomic signatures in microglial extracellular vesicles during acute inflammation: a gateway to neurological biomarkers

Nikita Ollen-Bittle[1], Wenxuan Wang[1], Kimberly Molina Bean[2,3], Shuang Zhao[2,3], Adriana Zardini Buzatto[2,3], Yifei Dong[4], Liang Li[2,3], Shawn N. Whitehead[1]

1 Department of Anatomy and Cell Biology, Schulich School of Medicine and Dentistry, Western University, London, Ontario, N6A 5C1

2 Department of Chemistry, University of Alberta, Edmonton, Alberta, T6G 2G2, Canada

3 The Metabolomics Innovation Centre (TMIC), University of Alberta, Edmonton, Alberta, T6G 2G2, Canada

4 Department of Biochemistry, Microbiology & Immunology, University of Saskatchewan, Saskatoon, Saskatchewan, Canada.

Corresponding Author:

Shawn Whitehead, PhD

Department of Anatomy and Cell Biology

454 Medical Sciences Building

The University of Western Ontario

London, Ontario

N6A 3K7

519 661-2111 x80440

shawn.whitehead@schulich.uwo.ca

Abstract

Extracellular vesicles (EVs) are membrane bound vesicles released from all cells throughout the body, including the central nervous system, and are known to carry both membrane-bound proteins and cargo reflective of their cell of origin. EVs show promise as neurological disease biomarkers due to their molecular makeup reflecting their parent-cell composition signature and due to their ability to cross the blood-brain barrier. To-date, the vast majority of research in this field has explored the protein profiles of EVs; however, lipids play an important role not only in the formation of EVs, but also in mediating cellular function and the pathological progression of many neurodegenerative conditions. Herein, we take a critical first step in determining the potential utility of EV lipids as biomarkers in neurological disease. *In vitro* we exposed BV-2 microglia to either control media or media containing lipopolysaccharides (LPS), a known pro-inflammatory stimulus, for 24 hours then isolated both the cells and their EVs and performed LC-MS/MS. For the first time, we reveal distinct lipidomic changes can differentiate resting vs. pro-inflammatory microglia and their EVs, while distinct lipids are preserved between EVs and their parent cell. Moreover, we add to current literature by demonstrating acute pro-inflammatory activation of microglia results in the activation and suppression of distinct lipidomic pathways. Finally, we demonstrate that analysis of lipid-based relationships between parent cells and their EVs may be a useful tool to infer cellular function. This study is the first of its kind to demonstrate that lipidomic analysis can not only differentiate the functional state of cells *in vitro* but can also differentiate their EVs. We lay the first brick in a foundation to support future research into EV lipids as novel and exciting biomarker candidates in neurological disease.

Keywords

Lipids, Biomarkers, LC-MS/MS, Microglia, Extracellular Vesicles, Lipidomics, neurological disease

Introduction

In addition to being a significant cause of both mortality and morbidity, neurological disease is one of the greatest strains on healthcare systems[1]. Due to the complexity of the nervous system, non-specific symptoms and variable presentations, neurological diseases are considered among the most difficult medical conditions to diagnose. Considering acute pathology, there are cases such as hemorrhagic vs ischemic stroke where conditions present almost indistinguishably clinically yet have opposing treatments that may worsen the alternative diagnosis[2]. In terms of chronic neurodegenerative diseases, there are cases where early intervention can significantly improve patient outcome such as early stem cell replacement therapy in specific leukodystrophies[3] or early commencement of cognitive enhancement therapeutics in Alzheimer's disease (AD)[4,5]. Thus, the ability to diagnose neurological diseases in their early phases is critical for identifying optimal therapeutic windows and effective treatments[6–8]. Research into biomarkers allowing for the early diagnosis of neurological conditions is continuously emerging. In AD a decrease in amyloid beta (Aβ) 42 has been shown to occur in CSF even prior to abnormal PET imaging[9,10] and a decrease in Aβ42/ Aβ40 within CSF shows promise as a potential diagnostic biomarker[11]. In the case of Parkinson's disease, Multiple Systems Atrophy and Dementia with Lewy Bodies α-synuclein decreases in CSF[8,12]. While these protein-based biomarkers show early promise, future work aims to utilize biomarker panels, in which additional biomarkers may help improve specificity. Additionally, since lumbar

puncture is invasive and not readily accessible outside of specialist centers, there is a need for blood-based biomarkers. Collectively, there is a dire and urgent need for the development of biomarkers to aid in the early diagnosis of neurological diseases.

Microglia are the predominant resident immune cell found in the parenchyma of the central nervous system (CNS) and are critical regulators of homeostasis and first responders to CNS injury. Microglia are known to play important roles in neuroprotective processes, but their dysregulation has also been associated with the progression of both acute CNS injury and neurodegenerative disease[13]. These cells display remarkable heterogeneity to various stimuli, rapidly transitioning between different phenotypes in response to environmental cues and pathological conditions[14]. Their unique ability to sense and respond to subtle changes in brain microenvironment makes them particularly valuable for early detection of neurological dysfunction. Recent single-cell transcriptomic studies have revealed distinct microglial subpopulations with disease-specific signatures, further emphasizing their potential as diagnostic indicators[15]. This makes microglia important targets for both understanding neurological diseases and for therapeutic modulation. In fact, in the last decade genome-wide association studies (GWAS) have identified genetic variants expressed in microglia that increase risk for late onset AD[16]. There has also been the emergence of microglia modulating therapeutics that are continuing to be explored in a therapeutic context including TREM2 and PPAR-γ agonists[17,18]. Collectively, since microglia are critical for the maintenance of homeostasis, can respond to but also exacerbate CNS injury and can potentially be modulated therapeutically, there is an increasing effort to discover blood-based microglia specific biomarkers as a peripheral window into neurological disease[19–21].

Lipids are dynamic organic molecules that make up more than half of the brains dry weight. They are essential components of cell membranes and axonal sheaths and take part in a vast range of requisite cellular processes in the brain including cell differentiation, energy storage, metabolism and cell signaling[22–25]. Lipid dysregulation is critically associated with several neurological diseases including AD, Parkinson's disease, multiple sclerosis (MS) and amyotrophic lateral sclerosis[26–28]. Given the need for biomarkers and the central role lipids play in CNS function, lipids make an intriguing candidate biomarker for many neurological diseases.

Extracellular vesicles (EVs) are small lipid membrane bound vesicles secreted by cells throughout the body and brain into extracellular fluids[29,30]. EVs were previously thought to be a mechanism of cellular waste removal; however, it is now known they are also important modulators of cell-to-cell signalling[29,30]. EVs are formed either through the outward budding of the cell membrane (microvesicles) or through the inward budding of the early endosomes as they mature into multivesicular bodies. These multivesicular bodies are then either targeted for destruction by the lysosome or for fusion with the cellular membrane releasing their content of small EVs (exosomes)[29]. Due to their mechanisms of formation, EVs contain membrane, membrane bound proteins and cargo from their parent cells[29–31]. Moreover, due to their small size and lipophilic nature, EVs are able to freely cross the blood brain barrier (BBB)[32,33]. The critical role of EVs in cellular communication, their composition being reflective of their parent cells and their ability to cross the BBB have caused EVs to quickly emerge as potential cell-specific biomarkers in neurological disease[34–36]. Most of the research on EV-based

biomarkers has focused on protein composition; however, lipids are known to be important players in EV-mediated cell-to-cell communication, cargo sorting and even functional effects on target cells[37]. New research on the potential of EV lipids as biomarkers is continuously emerging with recent reports of EV lipids showing promise as biomarkers for both breast[38] and prostate cancer[39]. Additionally, a recent study has shown dysregulation of lipids in EVs derived from post-mortem AD brains[40]. However, little is known about the baseline lipidomic profile of cell-specific EVs, how the EV lipidome relates to their cell of origin, or how/if it changes with changes in cell state. This is all requisite information if EV lipids are to be considered potential blood-based biomarkers for neurological disease and proof of principle work is needed in a controlled *in vitro* setting before moving to more complex experimental models and human samples.

Here, we interrogate the lipidomic profile of microglial EVs in a controlled setting to establish foundational information regarding the potential future utility of EV lipids as biomarkers in neurological disease. *In vitro,* we exposed BV-2 microglia to lipopolysaccharide (LPS), a component of gram-negative bacteria and well-established pro-inflammatory activator of microglia[41]. Following 24 hours we then isolated both the cells and their EVs released into the media and performed liquid chromatography– tandem mass spectrometry (LC-MS/MS). Notably, our findings indicate that the distinct lipidomic changes can differentiate LPS treated cells from non-treated cells and their EVs, while other lipid species are preserved between EVs and their parent cells. Moreover, we demonstrate acute pro-inflammatory activation of microglia results in the activation and suppression of distinct lipidomic pathways and show analysis of lipid ratios between parent cells and their EVs may be a useful tool to infer cellular function.

Collectively, this study marks the first of its kind to validate and encourage emerging research into EV lipids as novel and exciting potential biomarkers for neurological disease.

Methods

Cell growth conditions: BV-2 cells were donated from Dr. Tuan Trang at the University of Calgary. BV-2 cells were cultured in a humidified atmosphere at 37 °C with 5% CO_2. Prior to treatment cells were maintained with dulbecco's Modified Eagle Medium (DMEM) (Gibco) supplemented with 10% EV-depleted fetal bovine serum (FBS), Penicillin (100 U/mL) and Streptomycin (100 µg/mL) (Gibco). EV-depleted FBS was ultra-centrifuged at 100,000xG, 4 °C overnight after which the supernatant was filtered through a 0.2 µm filter.

Cell treatments: BV-2 microglia were seeded in 150 mm plates at a seeding density of 5.0×10^6 cells per plate and grown to 70% confluency. Cells were then washed with PBS and maintained in serum free media for 12 hours prior to treatment. Cells were then either treated with fresh serum free media (non-treated (NT), n=5) or 500 ng/ml LPS (n=5) in serum free media for 24 hours. At 24 hours both cells and their media were collected, frozen and transported on dry ice for further analysis. Media was collected into 50 mL tubes and cells were scraped off plates and collected in 15 mL tubes. The workflow utilized in this study is summarized in **Figure 1**.

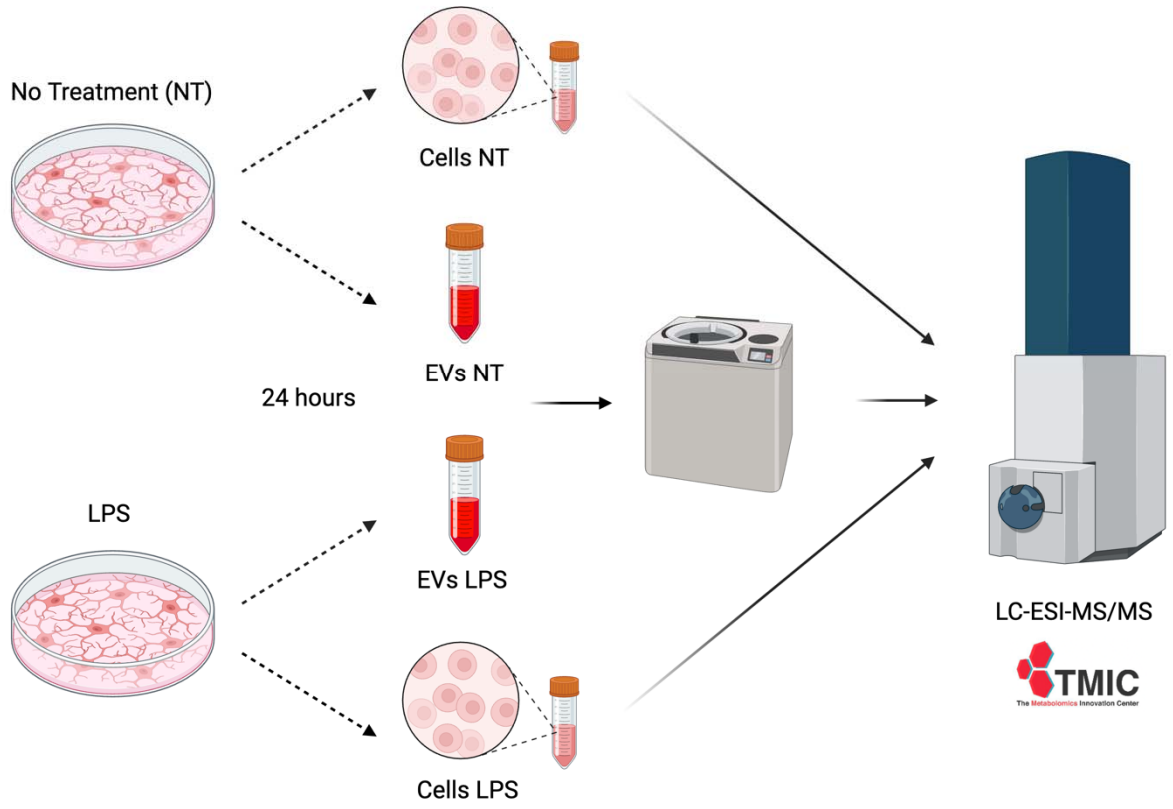

Figure 1. Workflow summary. BV-2 microglia were seeded in 150 mm plates and grown to 70% confluency. Cells were switched to serum free media for 12 hours then non-treated (NT) cells underwent fresh serum free media replacement (NT, n=5), while LPS exposed cells underwent media replacement with serum free media containing 500 ng/ml LPS (LPS, n=5). At 24 hours both cells and their media were collected and frozen. Once all samples were collected media was ultracentrifuged to isolate EVs and both cells and isolated EVs were sent to The Metabolomics Innovation Center (TMIC), Edmonton, Alberta, Canada for LC-MS/MS. Created with BioRender.com.

<u>EV isolation:</u> EVs were isolated as previously described[42]. Briefly, 50 mL tubes with collected media were centrifuged at 500 RCF for 5 minutes to pellet cellular debris before supernatant was immediately transferred to a new 50 mL tube and placed on ice. Supernatant was then filtered through a 0.2 µm SFPA into Amicon ultra 15 100k centrifuge filter tubes, which were centrifuged to achieve a final concentrated volume of 1 mL supernatant. Exosomes were then pelleted through ultracentrifugation of the concentrated supernatant at 50,000 rpm (MLA130

rotor) for 1 hour 15 minutes at 4°C. The supernatant was then removed, and the pellet was immediately dried, covered and placed on dry ice for shipment to the LC-MS/MS facility (TMIC, The Metabolomics Innovation Center, Edmonton, Alberta, Canada).

Data collection and processing by TMIC: Lipid isolation and LC-MS/MS data collection was performed in entirety at TMIC. Samples were analyzed randomized prior to analysis, and technicians at TMIC were blinded to sample group identities and other background information to reduce bias

Lipid extraction: Lipid extraction was performed based on a modified Folch liquid-liquid extraction protocol in cold conditions. Briefly, the samples were homogenized in 80% ice-cold methanol with ceramic beads (3.2 mm) at 4.6 m/s for 15 s. Samples were aliquoted to 20 nmol of TMC and then mixed with NovaMT LipidRep Internal Standard Basic Mix for Tissue/Cells (Catalog No. IDG-7002-IS). Samples were re-suspended in cold water and sonicated for 5 min. Phase separation was then performed by adding chilled dichloromethane and methanol to achieve a final solvent ratio of 2:1:0.7 (DCM:MeOH:water). The samples were vortexed and equilibrated at 4°C room temperature for 10 min and centrifuged at 16,000 g for 10 min at 4°C. The aqueous and organic layers were collected separately, evaporated to dryness under nitrogen, and stored at –80 °C for subsequent analyses.

To evaluate technical stability, an aggregate of Quality Control (QC) mixture was prepared by pooling aliquots for each the aqueous and organic layers from each sample, then splitting into multiple equal-volume aliquots. These aliquots were dried under nitrogen flow and stored at –

80 °C until use. For each randomized batch of samples (three batches of seven samples), one QC aliquot was re-suspended and duplicated injected, at the beginning and at the end of the batch sequence to evaluate batch effects. Additionally, multiple QC aliquots were injected both before and after all sample runs.

LC-MS Analysis: Dried extracts were re-suspended in mobile phase B, vortexed for 1 min, and diluted with mobile phase A. The LC-MS/MS was performed in both positive and negative ionization mode on a Thermo Vanquish UHPLC coupled to Bruker Impact II QTOF Mass Spectrometer. The system included a Waters Acquity CSH C18 column 1.7 µm, with a flow rate of 250 to 200 µL/min and a column oven temperature of 45°C. LC analysis was conducted using 10 mM ammonium formate in methanol/acetonitrile/water (50:40:10 v/v/v) as mobile phase A, and 10 mM ammonium formate in isopropanol/water (95:5 v/v) as mobile phase B. A 20-min gradient was employed, starting at 15% B at 0 min, 43% B at 2.0 min, 46% B at 6.3 min, 75% B at 10.4 min, 85% B at 10.6 min, 86% B at 10.8 min, 88% B at 13.5 min, and 98% B at 14.5 min, which was held until 15.0 min before allowing 5 min of column re-equilibration at the initial conditions. Injection volumes were 4.0 µL for positive ionization mode and 8.0 µL for negative ionization mode. Data were acquired in data-dependent acquisition mode over an m/z range of 150–2000, with MS/MS collision energies set between 10 and 60 eV.
Data Processing: LC-MS data from 25 injections per extract type (20 sample injection plus 5 QCs) were independently processed in positive and negative ionization using NovaMT LipidScreener software v 1.0.0. Positive- and negative- ion features were merged into a single feature-intensity matrix. Lipid identification was performed based on a three-tier identification approach based on MS/MS spectral similarity, retention time, and accurate mass: 1) Tier 1

(MS/MS): MS/MS match score ≥500; precursor m/z error ≤20.0 ppm and 5.0 mDa; 2) Tier 2 (MS/MS): MS/MS match score <500; precursor m/z error ≤20.0 ppm and 5.0 mDa; and 3) Tier 3 (MS): Mass match with m/z error ≤20.0 ppm and 5.0 mDa. Identified features from all tiers were used for normalization and statistical analysis. Lipids with identical identifications were summed prior to statistical analysis. Unidentified features were not employed for statistics. Identified features were normalized by internal standards and the median intensity ratio.

Statistical Analysis: Statistical analysis was performed using MetaboAnalyst 6.0 Software[43] without blinding. For multivariate statistics, features with near-constant values between the groups (the 25% features with the lowest relative standard deviation for all samples) were filtered out. The dataset was also auto-scaled. No other filtering, normalization, transformation, or scaling methods were employed before multivariate statistical analysis. For univariate statistics and pathways analysis, no extra filtering or data scaling methods were applied. For pathway analysis BioPAN software was used[44]. LipidLynxX[45] was first used to convert lipid names to BioPAN compatible bulk nomenclature. Due to the size of the dataset all non-BioPAN recognized lipid classes were removed, and pathway analysis was conducted within lipid categories without removing fatty acids. BioPAN groups included: Glycerophospholipids, glycerolipids and fatty acids. BioPAN software was then utilized for reaction pathway analysis at the species and class levels. For Cell:EV ratio analysis of distinct lipid species normality was assessed with a Shapiro-Wilk test then parametric and non-parametric data were analyzed with either an unpaired t-test or a Mann-Whitney test respectively. See **Table 1** for a full list of lipid subclass abbreviations utilized throughout this study.

Results

Lipid changes following 24 hours of either no treatment or LPS exposure of both microglia and their released EVs were assessed using LC-MS/MS. A total of 3626 lipid species were detected and identified. **Figure 2A** depicts the composition of lipid categories detected in this study. First, we assessed if the lipid profiles of detected and identified lipids could be used to differentiate the LPS exposed cells, NT cells and their respective EVs using multivariate statistics. Partial least squares discriminant analysis (PLS-DA) indicated that LPS treated microglia could be differentiated from NT microglia and their respective EVs by the component 1 (37.4%), and further by the component 2 (12%) (**Fig. 2B,C**). As shown in **Figure 2D**, further discrimination can be observed in the synchronized 3D plot demonstrating differentiation by three component analysis (component 1: 37.4%, component 2: 16%, component 3: 7.2 %) of treated and non-treated cells and their respective EVs. Component three variable importance in projection (VIP) scores from PLS-DA revealed PG 45:5;O, CerP 40:2;O2 and SHexCer 40:1;O to be the three lipids most important in differentiating the experimental groups (**Fig. 2E**). The model was evaluated using cross validation to assess predictive ability (Q2) and goodness of fit (R2), while permutation testing with 100 permutations, 3 components was applied to confirm the significance of the model. Model evaluation revealed a Q2 = 0.80893, R2 = 0.92105 and a p-value < 0.01 indicating that PLS-DA can differentiate LPS treated microglia, NT microglia and their respective EVs.

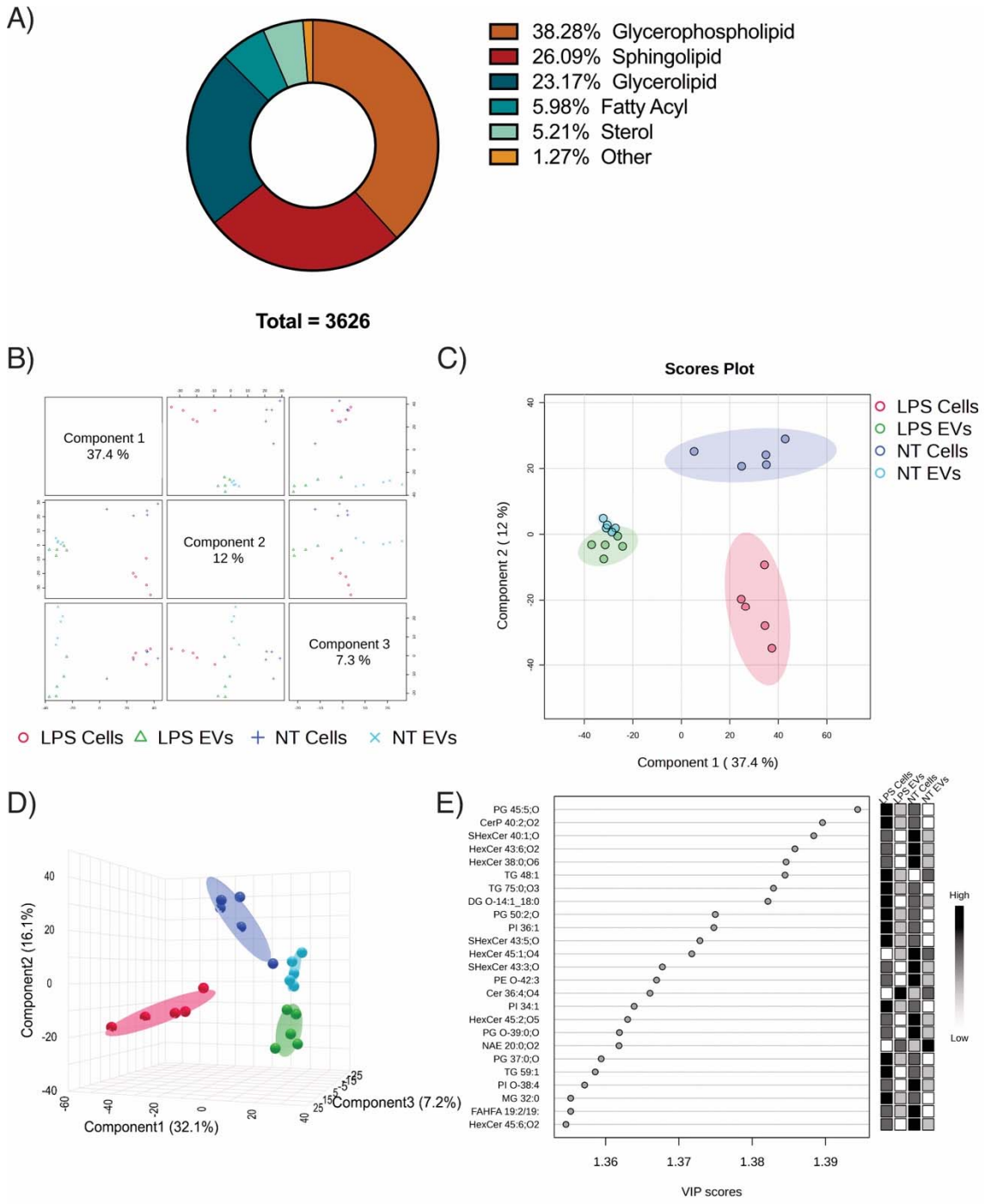

Figure 2. Untargeted lipidomic profiling can differentiate non-treated cells, LPS exposed cells and their respective EVs. A) Visual representation of lipid categories detected in this study. B) Three component partial least squares discriminant analysis (PLS-DA) overview. C) PLS-DA 2D scores plot shows complete differentiation of cell types with overlap of 95% confidence region between groups of EVs. D) Synchronized 3D plot demonstrating differentiation of treated and non-treated cells and their respective EVs. E) Component three variable importance in projection (VIP) plot showing the 25 most important lipids with grey scale-coloured boxes depicting the relative amount of each lipid in each experimental group.

Next, we aimed to interrogate distinct lipid changes in EV populations and how EVs correlated with their parent cells. First, we utilized an Euclidean heatmap with hierarchical clustering of 120 of the most important lipid species based on t-test/ANOVA comparison of groups which visualized distinct lipid changes in LPS treated cells and NT cells, as well as the EVs secreted from the LPS treated and NT cells **(Fig. 3A**). We further interrogated this finding by comparing the distinct cell groups, and their relation to their respective EVs. First, using volcano plots to visualize discrete lipid species varying between groups (all volcano plots utilized a fold change = 1.4 and a raw p-value threshold = 0.05) we compared LPS and NT cells. A total of 296 significantly decreased and 514 significantly increased lipid species were identified in LPS treated cells (**Fig. 3B**). We then assessed the discrete differences in the abundance of detected lipid species between both cell treatments and their EVs individually. Volcano plot analysis comparing NT EVs and NT cells identified 859 significantly decreased and 783 significantly increased lipid species in NT EVs (**Fig. 3C**); while, comparing LPS EVs relative to LPS cells revealed 1143 significantly decreased and 822 significantly increased lipid species in (**Fig. 3D**). We then aimed to assess if the overall lipidomic profile of EVs correlated with their parent cells. As visualized in a heatmap (**Fig. 3E**), spearman rank correlation indicated no correlation between groups of EVs and their parent cells. We next considered if there were distinct differences in the lipid profiles of EVs released from LPS treated cells relative to those released from NT cells. Volcano plot analysis identified 167 significantly decreased and 119 significantly increased lipid species in LPS EVs relative to NT EVs (**Fig. 3F**). To further interrogate these changes, we performed t-test analysis of all detected and identified lipid species between LPS and NT EVs. As shown in **Figure 3G**, this analysis identified 405 significantly altered lipids

between LPS EVs and NT EVs. The top 10 lipid classes found to significantly decrease in LPS EVs included: PI, HexCer, TG, Cer, PI-Cer, PE, DG, PIP, ST and MIPC (**Fig. 3H**). The top 10 lipid classes found to significantly increase in LPS EVs included: PI, PI-Cer, PIP, Cer, HexCer, MIPC, MG, DG, PE and TG (**Fig. 3I**).

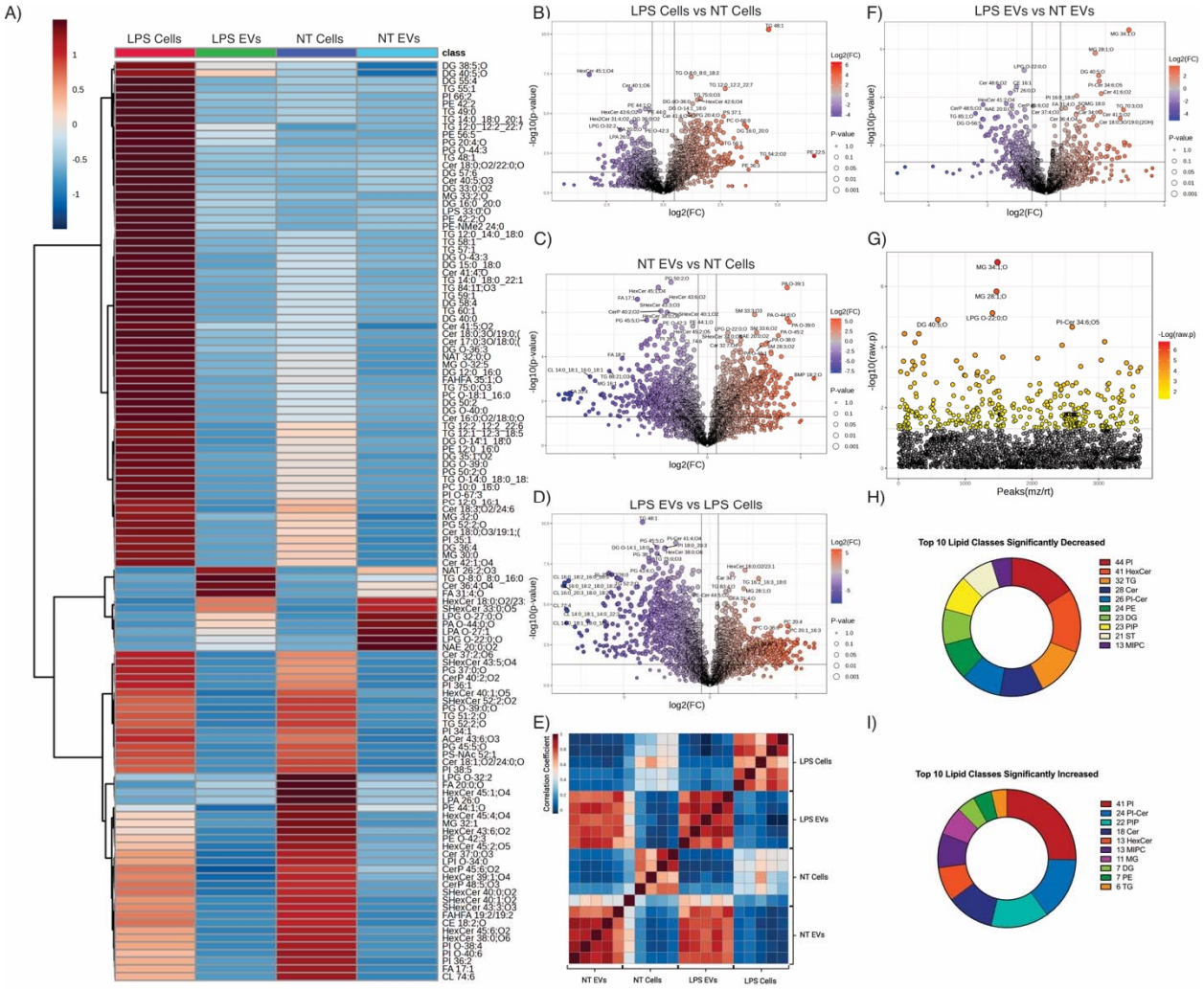

Figure 3. Distinct lipid species differentiate EVs from LPS exposed cells. A) Euclidean heatmap with hierarchical clustering of 120 of the most important lipid species based on t-test/ANOVA comparison of groups. B) Volcano plot analysis comparing LPS and NT Cells identified 296 significantly decreased and 514 significantly increased lipid species in LPS treated cells. Volcano plots all utilized a fold change threshold of 1.4 and a raw p-value threshold of 0.05. C) Volcano plot analysis comparing NT EVs and NT cells identified 859 significantly decrease and 783 significantly increased lipid species in NT EVs. D) Volcano plot analysis

identified 1143 significantly decreased and 822 significantly increased lipid species in LPS EVs relative to LPS cells. E) Spearman rank correlation heatmap. F) Volcano plot analysis identified 167 significantly decreased and 119 significantly increased lipid species in LPS EVs relative to NT EVs. G) Serial t-test analysis of all detected and identified lipid species identified 405 significantly altered lipids between LPS EVs and NT EVs. H) Visual representation of the top 10 lipid classes significantly decreased in LPS EVs compared to NT EVs based on t-test results depicted in G. I) Visual representation of the top 10 lipid significantly increased in LPS EVs compared to NT EVs based on t-test results depicted in G. Created with BioRender.com.

We then sought to determine if distinct lipid pathways were activated or suppressed in LPS exposed microglia relative to NT microglia. We conducted BioPAN analysis for reactions involving glycerophospholipids and glycerolipids at the class (**Fig. 4A,E,F**) and species (**Fig. 4. B,C**) level, and for fatty acids (**Fig. 4A,D**). **Table 2**. Summarizes the BioPAN results of all activated and suppressed reactions and the probable genes associated with these changes. Of note, at the class level for glycerolipids, results revealed an increase in DG and TG lipids. At the class level for glycerophospholipids, BioPAN analysis identified an increase in reactions producing Lyso-PS and LPA species with a decrease in LPC formation.

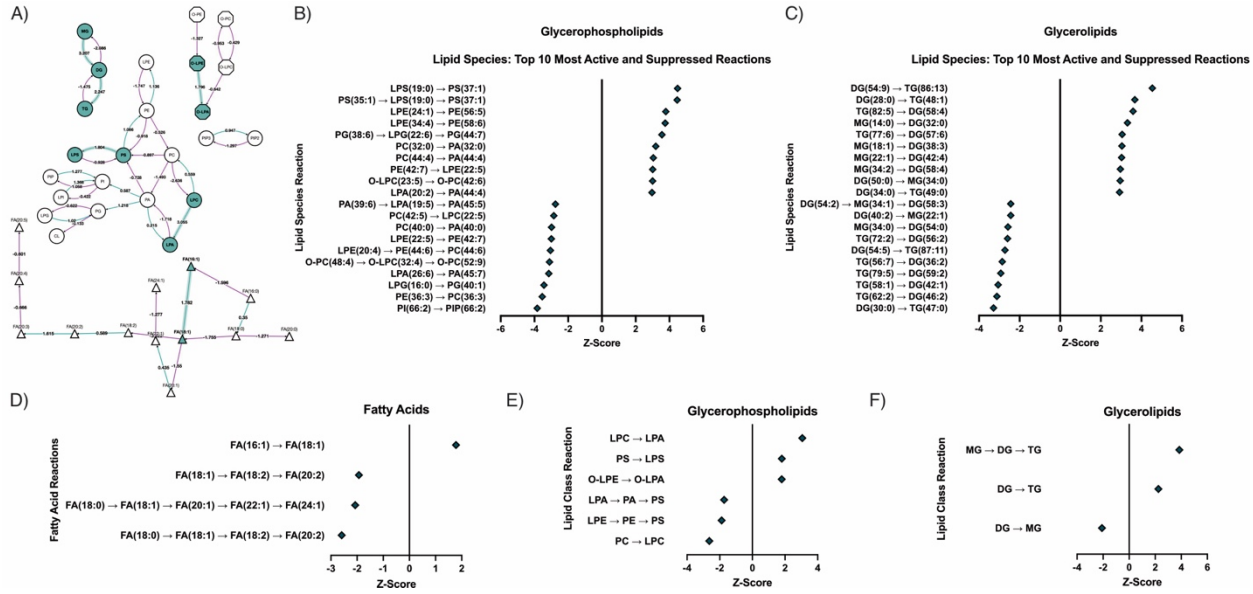

Figure 4. Distinct lipid reactions are activated and suppressed in LPS exposed cells. BioPAN analysis of lipid classes, lipid species and fatty acids revealed distinct reactions are activated and suppressed in LPS treated cells compared to NT cells. A) Diagram of activated reactions in lipid classes and fatty acids highlighted in green with respective Z-scores noted in reaction arrows. B) Top 10 activated and suppressed lipid reactions at the species level falling under the glycerophospholipid category. C) Top 10 activated and suppressed lipid reactions at the species level falling under the glycerolipid category. D) Activated and suppressed fatty acid reactions in LPS exposed cells. E) Most activated and suppressed lipid class reactions in the glycerophospholipid category. F) Most activated and suppressed lipid class reactions in the glycerolipid category. *LPS within this figure denotes the lipid class lysophosphatidylserines. See Table 1 For the entire list of lipid subclass abbreviations.

Given distinct lipid reactions are both activated and suppressed in LPS treated cells, we then decided to interrogate the relationship between cell treatments and their EVs through the Cell:EV ratio of species of interest. As shown in **Figure 5A**, Volcano plot analysis with a fold change threshold of 1.4 and a raw p-value threshold of 0.05 comparing LPS Cell:EV and NT Cell:EV ratios identified 179 significantly decreased and 397 significantly increased lipid ratios with LPS exposure. Further comparison through t-tests analysis comparing the Cell:EV ratio of all identified lipids in LPS and NT groups identified 582 lipids with significantly altered ratios (**Fig. 5B**). We then interrogated the ratio analysis of distinct lipid species thought to exert neurotoxic effects. The simple ganglioside species GM3 (d18:1/16:0) was among the lipid species

significantly increased (p = 0.0491) in the Cell:EV ratio of LPS treated cells (**Fig. 5C**). We further interrogated lyso-phosphatidylcholines (LPCs) and oxidized phosphatidylcholines (OxPCs). Two LPCs were identified to have significantly altered ratios in the LPS treated group. LPC 30:4 was found to have a significantly increased ratio with LPS treatment (**Fig. 5D);** while LPC 22:5 was found to have a significantly decreased (p = 0.0317) ratio with LPS treatment (**Fig. 5E**). Two OxPCs were also found to have altered ratios with LPS treatment. PC 30:0;O was found to have an increased ratio (p = 0.0360) with LPS treatment (**Fig. 5F**); while PC 43:11;O was shown to have a significantly decreased (p = 0.0079) ratio with LPS treatment (**Fig. 5G**).

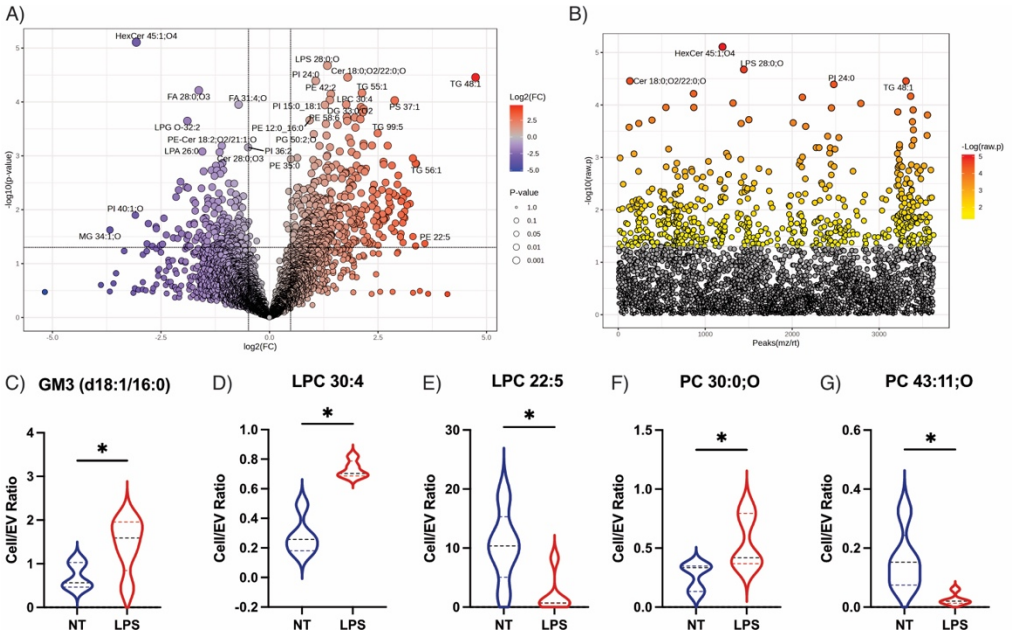

Figure 5. The Cell:EV ratio of distinct lipid species differs between LPS and non-treated cells. A) Volcano plot analysis with a fold change threshold of 1.4 and a raw p-value threshold of 0.05 comparing LPS Cell:EV and NT Cell:EV ratios identified 179 significantly decreased and 397 significantly increased lipid ratios with LPS treatment. B) T-tests comparing the Cell:EV ratio of all identified lipids in LPS and NT groups identified 582 lipids with significantly altered ratios. C) GM3 (d18:1/16:0) was among the lipid species significantly increased (p = 0.0491) in the Cell:EV ratio of LPS treated cells. D) Two significantly altered lyso-phosphatidylcholines (LPCs) were detected between treatments. LPC 30:4 was found to have a significantly increased ratio with LPS treatment; while, E) LPC 22:5 was found to have a significantly decreased (p = 0.0317) ratio with LPS treatment. F) Additionally, two OxPCs species were found to have altered ratios with LPS treatment. PC 30:0;O was found to have an increased ratio (p = 0.0360) with

LPS treatment; while, G) PC 43:11;O was shown to have a significantly decreased ($p = 0.0079$) ratio with LPS treatment.

Discussion

This study marks the first of its kind to interrogate the lipidomic relationship between microglia and their secreted EVs. The significance of this study is three-fold: 1) in a controlled *in vitro* experiment, we reveal that distinct lipidomic changes can differentiate microglia exposed to LPS from NT microglia and their EVs; while also demonstrating that distinct lipids are preserved, and others change with cell activation. Elucidating this relationship validates EV lipids as a potential future lipid-based biomarker capable of serving as a non-invasive window into changes in microglial function in the CNS. 2) We added to current literature on acute microglial activation with LPS by demonstrating acute pro-inflammatory activation of microglia results in the activation and suppression of distinct lipidomic pathways. This provides mechanistic insight into biological mechanisms and metabolic changes occurring with acute pro-inflammatory activation. Finally, 3) through analyzing the relationships between parent cells and their secreted EVs, we reveal lipid-specific changes and complex relationships within lipid classes in response to pro-inflammatory activation. These results demonstrate that lipid changes occurring with pro-inflammatory activation in microglia and their secreted EVs are highly complex and encourages future research investigating microglial/EV lipid changes with different experimental models and disease profiles. Collectively, this study utilized a controlled in vitro approach to elucidate foundational information on the lipidome of both microglia and their secreted EVs. This validates emerging research into EV lipids as novel and exciting potential biomarkers for neurological disease.

Through an untargeted approach and multi-variate analysis we were able to differentiate LPS-exposed BV-2 microglia, NT microglia and their respective EVs (**Fig. 2B-D**). **Figure 2E** demonstrates the top 25 most important lipids in differentiating these groups based on component 3 of PLS-DA which further differentiated EV groups. Of the top 25 lipids, 10 were noted to contain a ceramide backbone. Exosomes (small EVs) were likely the primary subtype of EVs captured in this study based on the EV isolation employing a 0.2 nm filter. In keeping with our results, exosomes have previously been shown to be ceramide-rich and ceramides have been shown to be responsible for triggering the budding of exosomes into MVBs[46]. Acute LPS exposure in macrophages has also been shown to increase ceramides[47] and a similar increase was recently observed in microglia[48]. We further interrogated the distinct lipid species changing between the experimental groups (**Fig. 3A,B**) and similarly found a prominent enrichment of distinct ceramide species in LPS treated microglia. Our results support ceramides as a critically important lipid for the differentiation of microglial activation phenotypes and their EVs.

From a neurological disease perspective accumulation of DG has also previously been shown in AD and PD brains[49–51]. DG lipids are known to serve as lipid mediators of immune activation[52] and are also precursors for major glycerophospholipids and TG lipids[53], potentially making both DG and TG lipids highly relevant in microglial activation. We found DG and TG lipids to be upregulated in LPS cells (**Fig. 3A,B**). This was further validated with BioPAN analysis (**Fig. 4A,C,F**) that revealed activated reactions metabolically shifting LPS treated cells towards TG synthesis. This was similarly shown in a recent publication utilizing a whole-cell matrix-assisted laser desorption/ionization (MALDI) MS whole cell fingerprinting

workflow[48]. Activated microglia also undergo alterations in mitochondrial function and the tricarboxylic acid cycle that can lead to TG accumulation within lipid droplets[54] and LPS treated microglia have been shown to accumulate TG-enriched lipid droplets[55], further validating our findings. Intriguingly, our results showed that while specific TG species increased in LPS treated cells, this was not preserved with an equal abundance in EVs. Compared to NT microglia, TG (48:1) was significantly increased in LPS treated cells (**Fig. 3A,B**); however, TG (48:1) was significantly lower in LPS treated EVs compared to LPS cells (**Fig. 3A,D**). This was in keeping with our correlation analysis (**Fig. 3E**) which showed no relationship between the overall lipidomic profile of EVs and their parent cells, and with our comparison between LPS EVs and NT EVs showing TG lipids as one of the top three lipid classes significantly decreased in LPS EVs (**Fig. 3G,H**). Collectively, our results suggest that rather than correlation of overall lipidomic profiles, distinct lipids species are preserved between EVs and their parent cells, while distinct species change based on cellular activation.

Utilizing BioPAN software to analyze glycerophospholipids, we identified an increase in reactions producing Lyso-PS and LPA species with a decrease in LPC formation. LPS stimulation has previously been shown to upregulate LPA production through Autotaxin (ATX), a phospholipase D that converts LPC into LPA[56]. This same pathway demonstrated activation based on our BioPAN analysis (**Fig. 4A**). Lyso-PS has also been shown to function in cellular morphology changes in microglia *in vitro*[57]. In contrast to our BioPAN analysis result however, previous work has shown an increase in distinct LPC species with LPS treatment of microglia[48]. It is important to note our overall dataset supports this as distinct LPC species were upregulated in LPS treated cells; however, this serves to highlight the importance of

pathway and reaction-based assessment of lipidomic data. Limitations of these results should also be considered, as currently BioPAN software does not factor in oxidized lipid species which may alter this finding. Future work especially when assessing disease specific paradigms should factor lipid oxidation into analysis.

To deepen our analysis, we examined the Cell:EV ratio of specific lipid species with known neurotoxic properties, including simple gangliosides, LPCs, and OxPCs[58–60]. Previous work has demonstrated GM3 colocalizes with plaques both in animal models[61,62] and in the AD brain[63,64]. OxPCs have also been shown to accumulate in MS lesions[58] and can be converted either through hydrolysis reactions or enzymatic processes to LPCs, which are known to cause demyelination and are even used as a means of inducing spinal cord injury in animal models[59]. We hypothesized that we may see a decrease in the Cell:EV ratio of these neurotoxic species in LPS treated cells as they take on a proinflammatory phenotype and accumulate lipids, potentially indicating reduced clearance through EVs. While we did see this relationship with GM3 (**Fig. 5C**), of the two LPCs and OxPCs identified to have significant differences with LPS treatment, LPC 30:4 and PC 30:0;O were found to have a significantly increased ratio with LPS treatment, while LPC 22:5 and PC 43:11;O were shown to have a significantly decreased ratios (**Fig. 5D-G**). This suggests a dynamic relationship of these neurotoxic species in which cell activation and lipid class are not the only influences on the Cell:EV ratio. It remains probable physiologically that the type of pro-inflammatory exposure, extracellular environment, genetics and chronicity of pro-inflammatory state all factor into the Cell:EV ratios of distinct lipid species. Future work should consider assessment of these relationships when characterizing cell-specific changes in EV lipids.

Additional limitations and future directions should also be noted. While EV lipids may one day be promising biomarkers for neurological diseases important logistical challenges exist. Analysis of EVs requires collection, isolation, extraction and analysis processes that may take too long to be useful depending on the clinical setting. For instance, with current technology EV lipids would not likely be useful for acutely differentiating stroke subtype in an emergency room setting, until technical advances improve the temporal limitations[34]. Additionally, this study serves as a critical foundation to a plethora of research to come before clinical utility even in more chronic conditions. Future research is needed to determine the effects of differential stimuli, different cell lines and primary cells, and different diseases both in experimental models and samples from human patients. This work provides foundational evidence to continue the pursuit of microglia lipid EV-based biomarkers in neurological disease.

Overall, this study provides the critical foundation requisite for the future study of lipid-based EV biomarkers in neurological diseases. For the first time, we validate that distinct lipid changes can differentiate LPS exposed microglia from NT microglia and their EVs; while demonstrating distinct lipids are preserved between the EVs and their parent cells, and others change with cell activation. Collectively, we validate a workflow for the *in vitro* characterization of EVs and most importantly demonstrate that microglial EV lipidome holds potential as a non-invasive window into functional changes in microglia.

Funding Sources

This study was supported by the Canadian Institutes for Health Research (CIHR) [202104PJT-461038] and the Natural Sciences and Engineering Research Council of Canada (NSERC) [RGPIN-2019-04742] to SNW. Additionally, NO and WW were supported by CIHR Canada Graduate Scholarships Doctoral Awards.

References

[1] GBD 2017 US Neurological Disorders Collaborators. Burden of Neurological Disorders Across the US From 1990-2017: A Global Burden of Disease Study. JAMA Neurol 2021;78:165–76. https://doi.org/10.1001/jamaneurol.2020.4152.
[2] Kase CS, Furlan AJ, Wechsler LR, Higashida RT, Rowley HA, Hart RG, et al. Cerebral hemorrhage after intra-arterial thrombolysis for ischemic stroke. Neurology 2001;57:1603. https://doi.org/10.1212/WNL.57.9.1603.
[3] Dulski J, Heckman MG, White LJ, Żur-Wyrozumska K, Lund TC, Wszolek ZK. Hematopoietic Stem Cell Transplantation in CSF1R-Related Leukoencephalopathy: Retrospective Study on Predictors of Outcomes. Pharmaceutics 2022;14. https://doi.org/10.3390/pharmaceutics14122778.
[4] Dubois B, Padovani A, Scheltens P, Rossi A, Dell'Agnello G, Saykin A. Timely Diagnosis for Alzheimer's Disease: A Literature Review on Benefits and Challenges. J Alzheimer's Dis 2016;49:617–31. https://doi.org/10.3233/JAD-150692.
[5] Vrahatis AG, Skolariki K, Krokidis MG, Lazaros K, Exarchos TP, Vlamos P. Revolutionizing the Early Detection of Alzheimer's Disease through Non-Invasive Biomarkers: The Role of Artificial Intelligence and Deep Learning. Sensors 2023;23. https://doi.org/10.3390/s23094184.
[6] Rasmussen J, and Langerman H. Alzheimer's Disease – Why We Need Early Diagnosis. Degener Neurol Neuromuscul Dis 2019;9:123–30. https://doi.org/10.2147/DNND.S228939.
[7] Miller JR. The importance of early diagnosis of multiple sclerosis. J Manag Care Pharm 2004;10:S4-11.
[8] Hansson O. Biomarkers for neurodegenerative diseases. Nat Med 2021;27:954–63. https://doi.org/10.1038/s41591-021-01382-x.
[9] Palmqvist S, Mattsson N, Hansson O, for the Alzheimer's Disease Neuroimaging Initiative. Cerebrospinal fluid analysis detects cerebral amyloid-β accumulation earlier than positron emission tomography. Brain 2016;139:1226–36. https://doi.org/10.1093/brain/aww015.
[10] Olsson B, Lautner R, Andreasson U, Öhrfelt A, Portelius E, Bjerke M, et al. CSF and blood biomarkers for the diagnosis of Alzheimer's disease: a systematic review and meta-analysis. Lancet Neurol 2016;15:673–84. https://doi.org/10.1016/S1474-4422(16)00070-3.
[11] Hansson O, Lehmann S, Otto M, Zetterberg H, Lewczuk P. Advantages and disadvantages of the use of the CSF Amyloid β (Aβ) 42/40 ratio in the diagnosis of Alzheimer's Disease. Alzheimers Res Ther 2019;11:34. https://doi.org/10.1186/s13195-019-0485-0.

[12] Parnetti L, Gaetani L, Eusebi P, Paciotti S, Hansson O, El-Agnaf O, et al. CSF and blood biomarkers for Parkinson's disease. Lancet Neurol 2019;18:573–86. https://doi.org/10.1016/S1474-4422(19)30024-9.
[13] Hickman S, Izzy S, Sen P, Morsett L, El Khoury J. Microglia in neurodegeneration. Nat Neurosci 2018;21:1359–69. https://doi.org/10.1038/s41593-018-0242-x.
[14] Tan Y-L, Yuan Y, Tian L. Microglial regional heterogeneity and its role in the brain. Mol Psychiatry 2020;25:351–67. https://doi.org/10.1038/s41380-019-0609-8.
[15] Olah M, Menon V, Habib N, Taga MF, Ma Y, Yung CJ, et al. Single cell RNA sequencing of human microglia uncovers a subset associated with Alzheimer's disease. Nat Commun 2020;11:6129. https://doi.org/10.1038/s41467-020-19737-2.
[16] Romero-Molina C, Garretti F, Andrews SJ, Marcora E, Goate AM. Microglial efferocytosis: Diving into the Alzheimer's disease gene pool. Neuron 2022;110:3513–33. https://doi.org/10.1016/j.neuron.2022.10.015.
[17] Lewcock JW, Schlepckow K, Di Paolo G, Tahirovic S, Monroe KM, Haass C. Emerging Microglia Biology Defines Novel Therapeutic Approaches for Alzheimer's Disease. Neuron 2020;108:801–21. https://doi.org/10.1016/j.neuron.2020.09.029.
[18] Carta AR, Pisanu A. Modulating Microglia Activity with PPAR-γ Agonists: A Promising Therapy for Parkinson's Disease? Neurotox Res 2013;23:112–23. https://doi.org/10.1007/s12640-012-9342-7.
[19] Zhang P-F, Hu H, Tan L, Yu J-T. Microglia Biomarkers in Alzheimer's Disease. Mol Neurobiol 2021;58:3388–404. https://doi.org/10.1007/s12035-021-02348-3.
[20] Chen K, Wang H, Ilyas I, Mahmood A, Hou L. Microglia and Astrocytes Dysfunction and Key Neuroinflammation-Based Biomarkers in Parkinson's Disease. Brain Sci 2023;13. https://doi.org/10.3390/brainsci13040634.
[21] Tirandi A, Sgura C, Carbone F, Montecucco F, Liberale L. Inflammatory biomarkers of ischemic stroke. Intern Emerg Med 2023;18:723–32. https://doi.org/10.1007/s11739-023-03201-2.
[22] Ioannou MS, Jackson J, Sheu S-H, Chang C-L, Weigel AV, Liu H, et al. Neuron-Astrocyte Metabolic Coupling Protects against Activity-Induced Fatty Acid Toxicity. Cell 2019;177:1522-1535.e14. https://doi.org/10.1016/j.cell.2019.04.001.
[23] Bazan NG. Lipid signaling in neural plasticity, brain repair, and neuroprotection. Mol Neurobiol 2005;32:89–103. https://doi.org/10.1385/MN:32:1:089.
[24] Montani L. Lipids in regulating oligodendrocyte structure and function. 1 Cell Dev Biol Bone Marrow Meriem Lamghari2 Role Lipids CNS Cell Physiol Pathol ByShyuan Ngo 2021;112:114–22. https://doi.org/10.1016/j.semcdb.2020.07.016.
[25] Bansal R, Winkler S, Bheddah S. Negative Regulation of Oligodendrocyte Differentiation by Galactosphingolipids. J Neurosci 1999;19:7913. https://doi.org/10.1523/JNEUROSCI.19-18-07913.1999.
[26] Phan K, He Y, Bhatia S, Pickford R, McDonald G, Mazumder S, et al. Multiple pathways of lipid dysregulation in amyotrophic lateral sclerosis. Brain Commun 2023;5:fcac340. https://doi.org/10.1093/braincomms/fcac340.
[27] Wei J, Wong LC, Boland S. Lipids as Emerging Biomarkers in Neurodegenerative Diseases. Int J Mol Sci 2024;25. https://doi.org/10.3390/ijms25010131.
[28] Podbielska M, O'Keeffe J, Pokryszko-Dragan A. New Insights into Multiple Sclerosis Mechanisms: Lipids on the Track to Control Inflammation and Neurodegeneration. Int J Mol Sci 2021;22. https://doi.org/10.3390/ijms22147319.

[29] Doyle LM, Wang MZ. Overview of Extracellular Vesicles, Their Origin, Composition, Purpose, and Methods for Exosome Isolation and Analysis. Cells 2019;8. https://doi.org/10.3390/cells8070727.
[30] Yáñez-Mó M, Siljander PR-M, Andreu Z, Bedina Zavec A, Borràs FE, Buzas EI, et al. Biological properties of extracellular vesicles and their physiological functions. J Extracell Vesicles 2015;4:27066. https://doi.org/10.3402/jev.v4.27066.
[31] Raposo G, Stoorvogel W. Extracellular vesicles: exosomes, microvesicles, and friends. J Cell Biol 2013;200:373–83. https://doi.org/10.1083/jcb.201211138.
[32] Perets N, Oron O, Herman S, Elliott E, Offen D. Exosomes derived from mesenchymal stem cells improved core symptoms of genetically modified mouse model of autism Shank3B. Mol Autism 2020;11:65. https://doi.org/10.1186/s13229-020-00366-x.
[33] Ramos-Zaldívar HM, Polakovicova I, Salas-Huenuleo E, Corvalán AH, Kogan MJ, Yefi CP, et al. Extracellular vesicles through the blood–brain barrier: a review. Fluids Barriers CNS 2022;19:60. https://doi.org/10.1186/s12987-022-00359-3.
[34] Ollen-Bittle N, Roseborough AD, Wang W, Wu JD, Whitehead SN. Mechanisms and Biomarker Potential of Extracellular Vesicles in Stroke. Biology 2022;11. https://doi.org/10.3390/biology11081231.
[35] Ollen-Bittle N, Roseborough AD, Wang W, Wu JD, Whitehead SN. Connecting cellular mechanisms and extracellular vesicle cargo in traumatic brain injury. Neural Regen Res 2024;19.
[36] Thompson AG, Gray E, Heman-Ackah SM, Mäger I, Talbot K, Andaloussi SE, et al. Extracellular vesicles in neurodegenerative disease — pathogenesis to biomarkers. Nat Rev Neurol 2016;12:346–57. https://doi.org/10.1038/nrneurol.2016.68.
[37] Fyfe J, Casari I, Manfredi M, Falasca M. Role of lipid signalling in extracellular vesicles-mediated cell-to-cell communication. Adv Extracell Vesicles Mediat Cell--Cell Commun Metab 2023;73:20–6. https://doi.org/10.1016/j.cytogfr.2023.08.006.
[38] Liu L, Kawashima M, Sugimoto M, Sonomura K, Pu F, Li W, et al. Discovery of lipid profiles in plasma-derived extracellular vesicles as biomarkers for breast cancer diagnosis. Cancer Sci 2023;114:4020–31. https://doi.org/10.1111/cas.15935.
[39] Brzozowski JS, Jankowski H, Bond DR, McCague SB, Munro BR, Predebon MJ, et al. Lipidomic profiling of extracellular vesicles derived from prostate and prostate cancer cell lines. Lipids Health Dis 2018;17:211. https://doi.org/10.1186/s12944-018-0854-x.
[40] Su H, Rustam YH, Masters CL, Makalic E, McLean CA, Hill AF, et al. Characterization of brain-derived extracellular vesicle lipids in Alzheimer’s disease. J Extracell Vesicles 2021;10:e12089. https://doi.org/10.1002/jev2.12089.
[41] Nakamura Y, Si QS, Kataoka K. Lipopolysaccharide-induced microglial activation in culture: temporal profiles of morphological change and release of cytokines and nitric oxide. Neurosci Res 1999;35:95–100. https://doi.org/10.1016/S0168-0102(99)00071-1.
[42] Roseborough AD, Zhu Y, Zhao L, Laviolette SR, Pasternak SH, Whitehead SN. Fibrinogen primes the microglial NLRP3 inflammasome and propagates pro-inflammatory signaling via extracellular vesicles: Implications for blood-brain barrier dysfunction. Neurobiol Dis 2023;177:106001. https://doi.org/10.1016/j.nbd.2023.106001.
[43] Pang Z, Lu Y, Zhou G, Hui F, Xu L, Viau C, et al. MetaboAnalyst 6.0: towards a unified platform for metabolomics data processing, analysis and interpretation. Nucleic Acids Res 2024;52:W398–406. https://doi.org/10.1093/nar/gkae253.

[44] Gaud C, C. Sousa B, Nguyen A, Fedorova M, Ni Z, O?Donnell V, et al. BioPAN: a web-based tool to explore mammalian lipidome metabolic pathways on LIPID MAPS [version 2; peer review: 3 approved]. F1000Research 2021;10. https://doi.org/10.12688/f1000research.28022.2.
[45] Ni Z, Fedorova M. LipidLynxX: a data transfer hub to support integration of large scale lipidomics datasets. bioRxiv 2020:2020.04.09.033894. https://doi.org/10.1101/2020.04.09.033894.
[46] Trajkovic K, Hsu C, Chiantia S, Rajendran L, Wenzel D, Wieland F, et al. Ceramide Triggers Budding of Exosome Vesicles into Multivesicular Endosomes. Science 2008;319:1244–7. https://doi.org/10.1126/science.1153124.
[47] MacKichan ML, DeFranco AL. Role of Ceramide in Lipopolysaccharide (LPS)-induced Signaling: LPS INCREASES CERAMIDE RATHER THAN ACTING AS A STRUCTURAL HOMOLOG *. J Biol Chem 1999;274:1767–75. https://doi.org/10.1074/jbc.274.3.1767.
[48] Blank M, Enzlein T, Hopf C. LPS-induced lipid alterations in microglia revealed by MALDI mass spectrometry-based cell fingerprinting in neuroinflammation studies. Sci Rep 2022;12:2908. https://doi.org/10.1038/s41598-022-06894-1.
[49] Wood PL, Cebak JE, Woltjer RL. Diacylglycerols as biomarkers of sustained immune activation in Proteinopathies associated with dementia. Clin Chim Acta 2018;476:107–10. https://doi.org/10.1016/j.cca.2017.11.009.
[50] Wood PL, Medicherla S, Sheikh N, Terry B, Phillipps A, Kaye JA, et al. Targeted Lipidomics of Fontal Cortex and Plasma Diacylglycerols (DAG) in Mild Cognitive Impairment and Alzheimer's Disease: Validation of DAG Accumulation Early in the Pathophysiology of Alzheimer's Disease. J Alzheimers Dis 2015;48:537–46. https://doi.org/10.3233/JAD-150336.
[51] Chan RB, Oliveira TG, Cortes EP, Honig LS, Duff KE, Small SA, et al. Comparative Lipidomic Analysis of Mouse and Human Brain with Alzheimer Disease*. J Biol Chem 2012;287:2678–88. https://doi.org/10.1074/jbc.M111.274142.
[52] Brose N, Betz A, Wegmeyer H. Divergent and convergent signaling by the diacylglycerol second messenger pathway in mammals. Curr Opin Neurobiol 2004;14:328–40. https://doi.org/10.1016/j.conb.2004.05.006.
[53] Coleman RA, Mashek DG. Mammalian Triacylglycerol Metabolism: Synthesis, Lipolysis, and Signaling. Chem Rev 2011;111:6359–86. https://doi.org/10.1021/cr100404w.
[54] Khatchadourian A, Bourque SD, Richard VR, Titorenko VI, Maysinger D. Dynamics and regulation of lipid droplet formation in lipopolysaccharide (LPS)-stimulated microglia. Biochim Biophys Acta BBA - Mol Cell Biol Lipids 2012;1821:607–17. https://doi.org/10.1016/j.bbalip.2012.01.007.
[55] Marschallinger J, Iram T, Zardeneta M, Lee SE, Lehallier B, Haney MS, et al. Lipid-droplet-accumulating microglia represent a dysfunctional and proinflammatory state in the aging brain. Nat Neurosci 2020;23:194–208. https://doi.org/10.1038/s41593-019-0566-1.
[56] Awada R, Saulnier-Blache JS, Grès S, Bourdon E, Rondeau P, Parimisetty A, et al. Autotaxin Downregulates LPS-Induced Microglia Activation and Pro-Inflammatory Cytokines Production. J Cell Biochem 2014;115:2123–32. https://doi.org/10.1002/jcb.24889.

[57] Tokizane K, Konishi H, Makide K, Kawana H, Nakamuta S, Kaibuchi K, et al. Phospholipid localization implies microglial morphology and function via Cdc42 in vitro. Glia 2017;65:740–55. https://doi.org/10.1002/glia.23123.
[58] Dong Y, D'Mello C, Pinsky W, Lozinski BM, Kaushik DK, Ghorbani S, et al. Oxidized phosphatidylcholines found in multiple sclerosis lesions mediate neurodegeneration and are neutralized by microglia. Nat Neurosci 2021;24:489–503. https://doi.org/10.1038/s41593-021-00801-z.
[59] Plemel JR, Michaels NJ, Weishaupt N, Caprariello AV, Keough MB, Rogers JA, et al. Mechanisms of lysophosphatidylcholine-induced demyelination: A primary lipid disrupting myelinopathy. Glia 2018;66:327–47. https://doi.org/10.1002/glia.23245.
[60] Wang WX, Whitehead SN. Imaging mass spectrometry allows for neuroanatomic-specific detection of gangliosides in the healthy and diseased brain. Analyst 2020;145:2473–81. https://doi.org/10.1039/C9AN02270H.
[61] Wang W, Myers SJ, Ollen-Bittle N, Whitehead SN. Elevation of ganglioside degradation pathway drives GM2 and GM3 within amyloid plaques in a transgenic mouse model of Alzheimer's disease. Neurobiol Dis 2025;205:106798. https://doi.org/10.1016/j.nbd.2025.106798.
[62] Kaya I, Zetterberg H, Blennow K, Hanrieder J. Shedding Light on the Molecular Pathology of Amyloid Plaques in Transgenic Alzheimer's Disease Mice Using Multimodal MALDI Imaging Mass Spectrometry. ACS Chem Neurosci 2018;9:1802–17. https://doi.org/10.1021/acschemneuro.8b00121.
[63] Ollen-Bittle N, Pejhan S, Pasternak SH, Keene CD, Zhang Q, Whitehead SN. Co-registration of MALDI-MSI and histology demonstrates gangliosides co-localize with amyloid beta plaques in Alzheimer's disease. Acta Neuropathol (Berl) 2024;147:105. https://doi.org/10.1007/s00401-024-02759-1.
[64] Michno W, Bowman A, Jha D, Minta K, Ge J, Koutarapu S, et al. Spatial Neurolipidomics at the Single Amyloid-β Plaque Level in Postmortem Human Alzheimer's Disease Brain. ACS Chem Neurosci 2024. https://doi.org/10.1021/acschemneuro.4c00006.

Tables

Classification (Category – Main Class – Subclass)	**Abbreviation**
Sphingolipids - Ceramides - Acylceramides	ACer
Glycerophospholipids - Glycerophosphoglycerols - Monoacylglycerophosphomonoradylglycerols	BMP
Fatty Acyls - Fatty esters - Fatty acyl carnitines	Car
Glycerophospholipids - Cytidine-5'-diphosphate (CDP)-Glycerols - CDP-diacylglycerols	CDP-DG
Sterol Lipids - Sterols - Steryl esters	CE
Sphingolipids - Ceramides - N-acylsphingosines (ceramides)	Cer
Sphingolipids - Ceramides - Ceramide 1-phosphates	CerP
Glycerophospholipids - Glycerophosphoglycerophosphoglycerols - Monoacylglycerophosphoglycerophosphomonoradylglycerols (Cardiolipins)	CL
Fatty Acyls - Fatty esters - Fatty acyl CoAs	CoA
Glycerolipids - Diradylglycerols - Diacylglycerols	DG
Glycerolipids - Other Glycerolipids (hydroxymethyl-choline)	DGCC

Glycerolipids - Glycosyldiradylglycerols – Glycosyldiacylglycerols (Digalactosyldiacylgylcerols)	DGDG
Glycerolipids - Glycosylmonoradylglycerols – Glycosylmonoacylglycerols (Digalactosylmonoacylgylcerols)	DGMG
Glycerolipids - Other Glycerolipids (trimethyl-alanine)	DGTA
Glycerolipids - Other Glycerolipids (trimethyl-homoserine)	DGTS
Fatty Acyls - Fatty Acids and Conjugates - Fatty acids	FA
Fatty Acyls - Fatty acyl glycosides - Fatty acyl glycosides of mono- and disaccharides	FAG
Fatty Acyls - Fatty esters - Fatty acid estolides	FAHFA
Fatty Acyls - Fatty aldehydes	FAL
Fatty Acyls - Fatty alcohols	FOH
Glycerolipids - Glycosyldiradylglycerols - Glycosyldiacylglycerols	GlcADG
Sphingolipids - Acidic glycosphingolipids - Glucuronosphingolipids	GlcCer
Glycerophospholipids - Glycosylglycerophospholipids - Diacylglycosylglycerophospholipids	Glc-GP
Glycerophospholipids - Other Glycerophospholipids	GP
Fatty Acyls - Hydrocarbons	HC
Sphingolipids - Glycosphingolipids - Hexosyl ceramides	HexCer
Sphingolipids - Glycosphingolipids - Hexosyl ceramides (2 hexosyl groups)	Hex2Cer
Sphingolipids - Glycosphingolipids - Hexosyl ceramides (3 hexosyl groups)	Hex3Cer
Sphingolipids - Glycosphingolipids - Hexosyl ceramides (4 hexosyl groups)	Hex4Cer
Sphingolipids - Glycosphingolipids - Hexosyl ceramides (5 hexosyl groups)	Hex5Cer
Sphingolipids - Glycosphingolipids - Hexosyl ceramides (6 hexosyl groups)	Hex6Cer
Sphingolipids - Glycosphingolipids - Hexosyl ceramides (7 hexosyl groups)	Hex7Cer
Sphingolipids - Glycosphingolipids - Hexosyl ceramides (8 hexosyl groups)	Hex8Cer
Sphingolipids - Glycosphingolipids - Hexosyl ceramides (9 hexosyl groups)	Hex9Cer
Sphingolipids - Glycosphingolipids - Hexosyl ceramides (10 hexosyl groups)	Hex10Cer
Sphingolipids - Glycosphingolipids - Hexosyl ceramides (11 hexosyl groups)	Hex11Cer
Sphingolipids - Glycosphingolipids - Hexosyl ceramides (12 hexosyl groups)	Hex12Cer
Sphingolipids - Glycosphingolipids - Hexosyl ceramides (13 hexosyl groups)	Hex13Cer
Sphingolipids - Glycosphingolipids - Hexosyl ceramides (14 hexosyl groups)	Hex14Cer
Sphingolipids - Glycosphingolipids - Hexosyl ceramides (15 hexosyl groups)	Hex15Cer
Sphingolipids - Glycosphingolipids - Hexosyl ceramides (20 hexosyl groups)	Hex20Cer
Sphingolipids - Neutral glycosphingolipids - Hexosyl sphingoid bases	HexSPB
Glycerophospholipids - Glycerophosphates - Monoacylglycerophosphates (lysophosphatidic acids)	LPA
Glycerophospholipids - Glycerophosphocholines - Monoacylglycerophosphocholines (lysophosphatidylcholines)	LPC
Glycerophospholipids - Glycerophosphoethanolamines - Monoacylglycerophosphoethanolamines (lysophosphatidylethanolamines)	LPE
Glycerophospholipids - Glycerophosphoglycerols - Monoacylglycerophosphoglycerol (lysophosphatidylglycerol)	LPG
Glycerophospholipids - Glycerophosphoinositols - Monoacylglycerophosphoinositols (lysophosphatidylinositols)	LPI
Glycerophospholipids - Glycerophosphoinositolglycans - N-acylglycerophosphoinositolglycans	LPIM
Glycerophospholipids - Glycerophosphoserines - Monoacylglycerophosphoserines (lysophosphatidylserines)	Lyso-PS in text LPS within Figure 4
Sphingolipids - Sphingoid bases - Lysosphingomyelins and lysoglycosphingolipids	LSM
Sphingolipids - Phosphosphingolipids - Ceramide phosphoinositols	M(IP)2C
Glycerolipids - Monoradylglycerols - Monoacylglycerols	MG

Glycerolipids - Glycosyldiradylglycerols – Glycosyldiacylglycerols (Monogalactosyldiacylgylcerols)	MGDG
Glycerolipids - Glycosylmonoradylglycerols - Glycosylmonoacylglycerols (Monogalactosylmonoacylgylcerols)	MGMG
Sphingolipids - Phosphosphingolipids - Ceramide phosphoinositols	MIPC
Fatty Acyls - Fatty Acids and Conjugates - Nitrogenated fatty acids (primary amides, N-acyl amides, fatty nitriles and others)	NA
Fatty Acyls - Fatty amides - N-acyl ethanolamines (endocannabinoids)	NAE
Glycerophospholipids - Glycerophosphoethanolamines - Diacylglycerophosphoethanolamines	NAPE
Fatty Acyls - Fatty amides - N-acyl amines (taurines)	NAT
Glycerophospholipids - Glycerophosphates – Diacylglycerophosphates (Phosphatidic Acids)	PA
Glycerophospholipids - Glycerophosphocholines – Diacylglycerophosphocholines (Phosphatidylcholines)	PC
Glycerophospholipids - Glycerophosphoethanolamines – Diacylglycerophosphoethanolamines (Phosphatidylethanolamines)	PE
Sphingolipids - Phosphosphingolipids - Ceramide phosphoethanolamines	PE-Cer
Glycerophospholipids - Other Glycerophospholipids	PE-isoK
Glycerophospholipids - Glycerophosphoethanolamines – Diacylglycerophosphoethanolamines (N-methylethanolamine or N,N-dimethylethanolamine)	PE-NMe
Glycerophospholipids - Glycerophosphoglycerols - Monoacylglycerophosphoglycerols (Phosphatidylglycerols)	PG
Glycerophospholipids - Glycerophosphoglycerophosphates - Diacylglycerophosphoglycerophosphates	PGP
Glycerophospholipids - Other Glycerophospholipids (sulfate)	PGS
Glycerophospholipids - Glycerophosphoinositols – Diacylglycerophosphoinositols (Phosphatidylinositols)	PI
Sphingolipids - Phosphosphingolipids - Ceramide phosphoinositols	PI-Cer
Glycerophospholipids - Glycerophosphoinositolglycans - Diacylglycerophosphoinositolglycans	PIM
Glycerophospholipids - Glycerophosphoinositol monophosphates	PIP
Polyketides	PK
Glycerophospholipids - Glycerophosphonocholines - Diacylglycerophosphonocholines	PnC
Glycerophospholipids - Glycerophosphonoethanolamines - Diacylglycerophosphonoethanolamines	PnE
Glycerophospholipids - Glyceropyrophosphates - Diacylglyceropyrophosphates	PPA
Prenol Lipids	PR
Glycerophospholipids - Glycerophosphoserines – Diacylglycerophosphoserines (Phosphatidylserines)	PS
Glycerophospholipids - Glycerophosphoserines - Triacylglycerophosphoserines	PS-NAc
Glycerophospholipids - Other Glycerophospholipids	PT
Sphingolipids - Other Sphingolipids - Sulfoceramides	SCer
Sphingolipids - Acidic glycosphingolipids - Sulfoglycosphingolipids (sulfatides)	SHexCer
Saccharolipids	SL
Glycerophospholipids - Glycerophosphoglycerols - Diacylglycerophosphomonoradylglycerols	SLBPA
Sphingolipids - Phosphosphingolipids - Ceramide phosphocholines (sphingomyelins)	SM
Sphingolipids - Sphingoid bases	SPB
Sphingolipids - Sphingoid bases - Sphingoid base-1 phosphates	SPBP
Glycerolipids - Glycosyldiradylglycerols – Glycosyldiacylglycerols (Sulfoquinovosyldiacylglycerols)	SQDG
Glycerolipids - Glycosylmonoradylglycerols – Glycosylmonoacylglycerols (Sulfoquinovosylmonoacylglycerols)	SQMG
Sterol Lipids	ST
Sphingolipids - Amphoteric glycosphingolipids - Sulfohexosyl sphingoid bases	SulfateHexSPB

Glycerolipids - Triradylglycerols - Triacylglycerols	TG
Fatty Acyls - Fatty esters - Wax esters and diesters	WE

Table 1. Lipid classifications and abbreviations used in study. The classification and shorthand notation of lipids followed the guidance of LipidMaps (https://www.lipidmaps.org/shorthand_nomenclature), MSDial (http://prime.psc.riken.jp/compms/msdial/lipidnomenclature.html), and Liebisch et al. J. Lipid Res. 2020, 61, 1–17 (DOI: https://doi.org/10.1194/jlr.S120001025) with the exception of lysophosphatidylserine. Since in the manuscript text LPS to refers to lipopolysaccharide, in-text reference to lysophosphatidylserine is abbreviated Lyso-PS. Please note text within figure 4 showcasing BioPAN results does utilize LPS to denote lysophosphatidylserines.

Glycerophospholipids		
Activated Reactions	**Z-score**	**Predicted Genes**
LPC→LPA	3.055	ENPP2
PS→LPS	1.804	PLA2G2E, PLA2G2A, PLA2G2F
O-LPE→O-LPA	1.796	PLD2
Suppressed Reactions	Z-score	Predicted genes
PC→LPC	2.636	PLA2G2E, PLA2G2A, PLA2G2D, PLA2G2F, PLA2G1B, PLA2G4A, PLA2G4B, PLA2G4C, PLA2G4D, PLA2G4E, PLA2G4F
LPE→PE→PS	1.884	MBOAT1, MBOAT2, LPCAT3, LPCAT4, PTDSS2
LPA→PA→PS	1.73	AGPAT1, AGPAT2, AGPAT3, AGPAT4, AGPAT5, CDS1, PTDSS1
Glycerolipids		
Activated Reactions	**Z-score**	**Predicted genes**
MG→DG→TG	3.857	MGAT, DGAT2
DG→TG	2.247	DGAT2
Suppressed Reactions	Z-score	Predicted genes
DG→MG	2.086	PNPLA2, PNPLA3
Fatty Acids		
Activated Reactions	**Z-score**	**Predicted genes**
FA(16:1) →FA(18:1)	1.782	ELOVL5, ELOVL6
Supressed Reactions	**Z-score**	**Predicted genes**
FA(18:0) →FA(18:1) →FA(18:2) →FA(20:2)	2.591	SCD1, FADS2, ELOVL5
FA(18:0) →FA(18:1) →FA(20:1) →FA(22:1) →FA(24:1)	2.074	SCD1, ELOVL3, ELOVL3, ELOVL3
FA(18:1) →FA(18:2) →FA(20:2)	1.933	FADS2, ELOVL5

Table 2. BioPAN analysis revealed activated and suppressed reactions in LPS treated microglia at the lipid class level. Analysis was conducted by lipid categories including glycerophospholipids, glycerolipids and fatty acids.

Supplementary Material

Note: all Z scores shown as absolute values reflecting either activated or suppressed pathways comparing LPS vs NT.

Glycerophospholipids **Lipid species active reaction** **(LPS vs NT)**		
Activated Reactions	**Z-score**	**Predicted genes**
LPS(19:0)->PS(37:1)	4.486	MBOAT1, LPCAT3, LPCAT4
PS(35:1)->LPS(19:0)->PS(37:1)	4.462	PLA2G2E, PLA2G2A, PLA2G2F, MBOAT1, LPCAT3, LPCAT4
LPG(18:1)->PG(38:6)->LPG(22:6)->PG(44:7)	4.055	LPGAT1, CRLS1, PLA2G4D, PLA2G4F, CRLS1, LPGAT1, CRLS1
LPE(24:1)->PE(56:5)	3.786	MBOAT1, MBOAT2, LPCAT3, LPCAT4
LPE(34:4)->PE(58:6)	3.751	MBOAT1, MBOAT2, LPCAT3, LPCAT4
PG(38:6)->LPG(22:6)->PG(44:7)	3.556	PLA2G4D, PLA2G4F, CRLS1, LPGAT1, CRLS1
LPG(18:1)->PG(38:6)->LPG(22:6)->PG(39:7)	3.414	LPGAT1, CRLS1, PLA2G4D, PLA2G4F, CRLS1, LPGAT1, CRLS1
LPG(18:1)->PG(38:6)->LPG(22:6)->PG(38:7)	3.341	LPGAT1, CRLS1, PLA2G4D, PLA2G4F, CRLS1, LPGAT1, CRLS1
PC(32:0)->PA(32:0)	3.192	PLD1, PLD2
LPG(18:1)->PG(38:6)->LPG(22:6)->PG(40:8)	3.166	LPGAT1, CRLS1, PLA2G4D, PLA2G4F, CRLS1, LPGAT1, CRLS1
PC(44:4)->PA(44:4)	3.048	PLD1, PLD2
PE(34:0)->LPE(18:0)->PE(42:2)	3.031	PLA2G4C, MBOAT1, MBOAT2, LPCAT3, LPCAT4
PE(42:7)->LPE(22:5)	3.009	PLA2G4C
O-LPC(23:5)->O-PC(42:6)	3.004	LPCAT1
LPA(20:2)->PA(44:4)	2.97	AGPAT1, AGPAT2, AGPAT3, AGPAT4, AGPAT5
O-LPC(31:3)->O-PC(46:3)	2.952	LPCAT1
PC(39:2)->PA(39:2)	2.814	PLD1, PLD2
PG(38:6)->LPG(22:6)->PG(39:7)	2.771	PLA2G4D, PLA2G4F, CRLS1, LPGAT1, CRLS1
PIP(66:2)->PI(66:2)	2.734	SYNJ1, SYNJ2, SACM1L, MTMR1, MTMR2, MTMR3, MTMR4, MTMR6, MTMR7, MTMR8,

		MTMR9, MTMR14, PTEN
PE(44:2)->PC(44:2)	2.706	PEMT
PE(42:5)->PC(42:5)	2.682	PEMT
PG(38:6)->LPG(22:6)->PG(38:7)	2.681	PLA2G4D, PLA2G4F, CRLS1, LPGAT1, CRLS1
LPA(26:0)->PA(48:1)->LPA(32:1)	2.68	AGPAT1, AGPAT2, AGPAT3, AGPAT4, AGPAT5, PLA2G4A, PLA2G4D, PLA2G4E, PLA2G4F
LPG(18:1)->PG(38:6)->LPG(22:6)->PG(40:7)	2.657	LPGAT1, CRLS1, PLA2G4D, PLA2G4F, CRLS1, LPGAT1, CRLS1
PE(40:6)->PC(40:6)	2.612	PEMT
LPG(18:1)->PG(38:6)->LPG(22:6)->PG(42:6)	2.57	LPGAT1, CRLS1, PLA2G4D, PLA2G4F, CRLS1, LPGAT1, CRLS1
LPI(18:0)->PI(33:1)	2.568	MBOAT7
PE(42:0)->PC(42:0)	2.54	PEMT
LPC(18:1)->LPA(18:1)	2.535	ENPP2
PE(34:0)->LPE(16:0)	2.532	PLA2G4C
LPC(16:0)->PC(36:0)	2.52	LPCAT1, LPCAT2, LPCAT3, LPCAT4
LPA(17:0)->PA(32:0)	2.511	AGPAT1, AGPAT2, AGPAT3, AGPAT4, AGPAT5
O-LPC(31:3)->O-PC(48:3)	2.495	LPCAT1
LPC(18:1)->PC(44:1)	2.489	LPCAT1, LPCAT2, LPCAT3, LPCAT4
PG(38:6)->LPG(22:6)->PG(40:8)	2.466	PLA2G4D, PLA2G4F, CRLS1, LPGAT1, CRLS1
LPC(20:1)->LPA(20:1)->PA(39:2)	2.443	ENPP2, AGPAT1, AGPAT2, AGPAT3, AGPAT4, AGPAT5
PS(36:2)->PE(36:2)->LPE(20:1)->PE(46:1)	2.442	PISD, PLA2G4C, MBOAT1, MBOAT2, LPCAT3, LPCAT4
LPI(18:0)->PI(35:1)	2.416	MBOAT7
LPC(20:1)->PC(44:3)->PA(44:3)->LPA(24:3)->PA(48:4)	2.396	LPCAT1, LPCAT2, LPCAT3, LPCAT4, PLD1, PLD2, PLA2G4A, PLA2G4D, PLA2G4E, PLA2G4F, AGPAT1, AGPAT2, AGPAT3, AGPAT4, AGPAT5
LPC(20:1)->PC(46:1)->LPC(30:0)->PC(49:2)->LPC(33:2)	2.372	LPCAT1, LPCAT2, LPCAT3, LPCAT4, PLA2G2E, PLA2G2A, PLA2G2D, PLA2G2F, PLA2G1B, PLA2G4A, PLA2G4B, PLA2G4C, PLA2G4D, PLA2G4E, PLA2G4F, LPCAT1, LPCAT2, LPCAT3, LPCAT4, PLA2G2E, PLA2G2A, PLA2G2D, PLA2G2F, PLA2G1B, PLA2G4A, PLA2G4B, PLA2G4C, PLA2G4D, PLA2G4E, PLA2G4F
PA(36:2)->PI(36:2)	2.368	CDS1, CDS2, CDIPT
LPG(22:6)->PG(44:7)	2.361	LPGAT1, CRLS1
LPA(19:5)->PA(39:6)	2.353	AGPAT1, AGPAT2, AGPAT3, AGPAT4, AGPAT5
PE(28:1)->PC(28:1)	2.307	PEMT
PS(38:0)->PE(38:0)	2.265	PISD

PC(37:1)->PS(37:1)	2.257	PTDSS1
LPC(20:1)->PC(40:6)	2.256	LPCAT1, LPCAT2, LPCAT3, LPCAT4
LPG(18:1)->PG(42:2)	2.254	LPGAT1, CRLS1
LPC(20:1)->LPA(20:1)->PA(39:3)	2.248	ENPP2, AGPAT1, AGPAT2, AGPAT3, AGPAT4, AGPAT5
LPE(16:1)->PE(34:3)	2.233	MBOAT1, MBOAT2, LPCAT3, LPCAT4
LPC(18:2)->LPA(18:2)	2.232	ENPP2
PE(42:7)->LPE(22:6)	2.231	PLA2G4C
LPA(20:2)->PA(46:2)	2.216	AGPAT1, AGPAT2, AGPAT3, AGPAT4, AGPAT5
PS(42:1)->PE(42:1)->PC(42:1)	2.208	PISD, PEMT
LPE(36:3)->PE(54:3)	2.205	MBOAT1, MBOAT2, LPCAT3, LPCAT4
LPA(26:0)->PA(42:0)	2.203	AGPAT1, AGPAT2, AGPAT3, AGPAT4, AGPAT5
PE(34:0)->LPE(18:0)->PE(38:5)	2.199	PLA2G4C, MBOAT1, MBOAT2, LPCAT3, LPCAT4
LPG(18:1)->PG(42:3)	2.195	LPGAT1, CRLS1
LPE(36:3)->PE(56:7)	2.19	MBOAT1, MBOAT2, LPCAT3, LPCAT4
LPG(18:1)->PG(38:6)->LPG(22:6)->PG(42:9)	2.17	LPGAT1, CRLS1, PLA2G4D, PLA2G4F, CRLS1, LPGAT1, CRLS1
LPE(24:1)->PE(54:6)	2.156	MBOAT1, MBOAT2, LPCAT3, LPCAT4
LPE(18:0)->PE(42:2)	2.152	MBOAT1, MBOAT2, LPCAT3, LPCAT4
LPI(18:1)->PI(36:3)	2.14	MBOAT7
LPA(26:0)->PA(44:0)	2.139	AGPAT1, AGPAT2, AGPAT3, AGPAT4, AGPAT5
LPG(18:1)->PG(38:2)	2.098	LPGAT1, CRLS1
LPE(12:0)->PE(36:2)->LPE(20:1)->PE(46:1)	2.089	MBOAT1, MBOAT2, LPCAT3, LPCAT4, PLA2G4C, MBOAT1, MBOAT2, LPCAT3, LPCAT4
PA(35:1)->PI(35:1)	2.061	CDS1, CDS2, CDIPT
LPC(20:3)->LPA(20:3)	2.052	ENPP2
LPC(16:1)->PC(42:1)	2.028	LPCAT1, LPCAT2, LPCAT3, LPCAT4
LPI(18:1)->PI(35:2)	1.98	MBOAT7
PE(38:4)->PC(38:4)	1.972	PEMT
LPC(15:1)->PC(33:3)	1.923	LPCAT1, LPCAT2, LPCAT3, LPCAT4
LPC(16:0)->PC(42:0)	1.913	LPCAT1, LPCAT2, LPCAT3, LPCAT4
PA(35:0)->PG(35:0)	1.899	CDS1, CDS2, PTPMT1
PS(34:1)->PE(34:1)	1.888	PISD
PE(44:0)->PC(44:0)	1.887	PEMT
PS(40:2)->PE(40:2)	1.856	PISD
PG(38:6)->LPG(22:6)->PG(40:7)	1.843	PLA2G4D, PLA2G4F, CRLS1, LPGAT1, CRLS1

PE(42:3)->LPE(22:1)->PE(54:5)->LPE(38:5)	1.841	PLA2G4C, MBOAT1, MBOAT2, LPCAT3, LPCAT4, PLA2G4C
LPG(18:1)->PG(33:2)	1.838	LPGAT1, CRLS1
PS(35:1)->LPS(19:0)->PS(43:1)	1.824	PLA2G2E, PLA2G2A, PLA2G2F, MBOAT1, LPCAT3, LPCAT4
LPC(16:0)->PC(33:0)	1.82	LPCAT1, LPCAT2, LPCAT3, LPCAT4
PG(54:4)->LPG(34:1)	1.804	PLA2G4D, PLA2G4F, CRLS1
LPE(34:5)->PE(56:6)	1.786	MBOAT1, MBOAT2, LPCAT3, LPCAT4
PC(30:0)->PA(30:0)->PG(30:0)	1.771	PLD1, PLD2, CDS1, CDS2, PTPMT1
LPC(22:2)->LPA(22:2)->PA(42:5)	1.759	ENPP2, AGPAT1, AGPAT2, AGPAT3, AGPAT4, AGPAT5
PE(36:0)->PC(36:0)	1.75	PEMT
PA(35:2)->PI(35:2)	1.746	CDS1, CDS2, CDIPT
LPE(36:3)->PE(56:8)	1.745	MBOAT1, MBOAT2, LPCAT3, LPCAT4
PS(38:2)->LPS(22:1)	1.744	PLA2G2E, PLA2G2A, PLA2G2F
PG(38:6)->LPG(22:6)->PG(42:6)	1.737	PLA2G4D, PLA2G4F, CRLS1, LPGAT1, CRLS1
PA(28:0)->PG(28:0)	1.729	CDS1, CDS2, PTPMT1
PA(44:3)->LPA(24:3)	1.714	PLA2G4A, PLA2G4D, PLA2G4E, PLA2G4F
LPA(17:0)->PA(41:1)	1.705	AGPAT1, AGPAT2, AGPAT3, AGPAT4, AGPAT5
PA(36:1)->PI(36:1)	1.675	CDS1, CDS2, CDIPT
PE(38:1)->PC(38:1)	1.664	PEMT
LPC(32:1)->LPA(32:1)	1.655	ENPP2
LPG(18:1)->PG(38:5)	1.646	LPGAT1, CRLS1
Suppressed Reactions	**Z-score**	**Predicted genes**
PI(66:2)->PIP(66:2)	3.834	PI4KA, PI4K2A, PI4K2B, PIP5K1A, PIP5K1B, SACM1L
PE(36:3)->PC(36:3)	3.54	PEMT
LPG(16:0)->PG(40:1)	3.435	LPGAT1, CRLS1
LPA(26:6)->PA(45:7)	3.151	AGPAT1, AGPAT2, AGPAT3, AGPAT4, AGPAT5
O-PC(48:4)->O-LPC(32:4)->O-PC(52:9)	3.106	PLA2G2E, PLA2G2A, PLA2G2D, PLA2G2F, PLA2G1B, PLA2G4A, PLA2G4B, PLA2G4C, PLA2G4D, PLA2G4E, PLA2G4F, LPCAT1
LPE(20:4)->PE(44:6)->PC(44:6)	3.054	MBOAT1, MBOAT2, LPCAT3, LPCAT4, PEMT
LPE(22:5)->PE(42:7)	3	MBOAT1, MBOAT2, LPCAT3, LPCAT4
PC(40:0)->PA(40:0)	2.984	PLD1, PLD2
PC(42:5)->LPC(22:5)	2.85	PLA2G2E, PLA2G2A, PLA2G2D, PLA2G2F, PLA2G1B, PLA2G4A, PLA2G4B, PLA2G4C,

		PLA2G4D, PLA2G4E, PLA2G4F
PA(39:6)->LPA(19:5)->PA(45:5)	2.758	PLA2G4A, PLA2G4D, PLA2G4E, PLA2G4F, AGPAT1, AGPAT2, AGPAT3, AGPAT4, AGPAT5
PA(48:4)->LPA(32:3)	2.666	PLA2G4A, PLA2G4D, PLA2G4E, PLA2G4F
LPE(20:1)->PE(40:6)->PS(40:6)	2.662	MBOAT1, MBOAT2, LPCAT3, LPCAT4, PTDSS2
LPI(17:4)->PI(39:5)	2.652	MBOAT7
LPC(18:0)->PC(42:2)->LPC(20:1)	2.632	LPCAT1, LPCAT2, LPCAT3, LPCAT4, PLA2G2E, PLA2G2A, PLA2G2D, PLA2G2F, PLA2G1B, PLA2G4A, PLA2G4B, PLA2G4C, PLA2G4D, PLA2G4E, PLA2G4F
PE(42:2)->PC(42:2)->LPC(20:1)	2.579	PEMT, PLA2G2E, PLA2G2A, PLA2G2D, PLA2G2F, PLA2G1B, PLA2G4A, PLA2G4B, PLA2G4C, PLA2G4D, PLA2G4E, PLA2G4F
LPE(16:0)->PE(34:2)->PC(34:2)	2.576	MBOAT1, MBOAT2, LPCAT3, LPCAT4, PEMT
PE(34:3)->PC(34:3)	2.521	PEMT
O-LPC(18:0)->O-PC(42:1)->O-LPC(24:0)	2.519	LPCAT1, PLA2G2E, PLA2G2A, PLA2G2D, PLA2G2F, PLA2G1B, PLA2G4A, PLA2G4B, PLA2G4C, PLA2G4D, PLA2G4E, PLA2G4F
LPC(18:0)->PC(42:2)->LPC(22:2)	2.481	LPCAT1, LPCAT2, LPCAT3, LPCAT4, PLA2G2E, PLA2G2A, PLA2G2D, PLA2G2F, PLA2G1B, PLA2G4A, PLA2G4B, PLA2G4C, PLA2G4D, PLA2G4E, PLA2G4F
PE(42:2)->PC(42:2)->LPC(22:2)	2.427	PEMT, PLA2G2E, PLA2G2A, PLA2G2D, PLA2G2F, PLA2G1B, PLA2G4A, PLA2G4B, PLA2G4C, PLA2G4D, PLA2G4E, PLA2G4F
LPE(20:1)->PE(44:3)	2.423	MBOAT1, MBOAT2, LPCAT3, LPCAT4
PE(46:1)->PC(46:1)->LPC(28:1)	2.401	PEMT, PLA2G2E, PLA2G2A, PLA2G2D, PLA2G2F, PLA2G1B, PLA2G4A, PLA2G4B, PLA2G4C, PLA2G4D, PLA2G4E, PLA2G4F
PE(28:0)->PC(28:0)->PA(28:0)	2.354	PEMT, PLD1, PLD2
LPE(20:3)->PE(40:7)	2.324	MBOAT1, MBOAT2, LPCAT3, LPCAT4
PE(36:2)->PC(36:2)->PS(36:2)	2.321	PEMT, PTDSS1
LPC(18:0)->PC(42:2)->LPC(22:1)->PC(46:2)	2.268	LPCAT1, LPCAT2, LPCAT3, LPCAT4, PLA2G2E, PLA2G2A, PLA2G2D, PLA2G2F, PLA2G1B, PLA2G4A, PLA2G4B, PLA2G4C, PLA2G4D, PLA2G4E, PLA2G4F, LPCAT1, LPCAT2, LPCAT3, LPCAT4
PA(39:6)->LPA(19:5)->PA(43:6)->PS(43:6)	2.262	PLA2G4A, PLA2G4D, PLA2G4E, PLA2G4F, AGPAT1, AGPAT2, AGPAT3, AGPAT4, AGPAT5, CDS1, PTDSS1
LPE(16:1)->PE(38:2)->PS(38:2)->LPS(18:1)->PS(40:2)	2.256	MBOAT1, MBOAT2, LPCAT3, LPCAT4, PTDSS2, PLA2G2E, PLA2G2A, PLA2G2F, MBOAT1, LPCAT3, LPCAT4

LPC(18:0)->PC(42:2)->LPC(26:2)	2.244	LPCAT1, LPCAT2, LPCAT3, LPCAT4, PLA2G2E, PLA2G2A, PLA2G2D, PLA2G2F, PLA2G1B, PLA2G4A, PLA2G4B, PLA2G4C, PLA2G4D, PLA2G4E, PLA2G4F
LPC(20:0)->PC(40:4)->PS(40:4)	2.23	LPCAT1, LPCAT2, LPCAT3, LPCAT4, PTDSS1
PE(42:2)->PC(42:2)->LPC(22:1)->PC(46:2)	2.225	PEMT, PLA2G2E, PLA2G2A, PLA2G2D, PLA2G2F, PLA2G1B, PLA2G4A, PLA2G4B, PLA2G4C, PLA2G4D, PLA2G4E, PLA2G4F, LPCAT1, LPCAT2, LPCAT3, LPCAT4
LPA(26:6)->PA(45:8)	2.223	AGPAT1, AGPAT2, AGPAT3, AGPAT4, AGPAT5
PC(49:2)->LPC(31:0)	2.22	PLA2G2E, PLA2G2A, PLA2G2D, PLA2G2F, PLA2G1B, PLA2G4A, PLA2G4B, PLA2G4C, PLA2G4D, PLA2G4E, PLA2G4F
PE(36:2)->PC(36:2)->PA(36:2)->PS(36:2)	2.216	PEMT, PLD1, PLD2, CDS1, PTDSS1
PE(36:2)->PC(36:2)->PA(36:2)->PG(36:2)	2.208	PEMT, PLD1, PLD2, CDS1, CDS2, PTPMT1
PA(42:0)->LPA(26:0)	2.203	PLA2G4A, PLA2G4D, PLA2G4E, PLA2G4F
PE(42:2)->PC(42:2)->LPC(26:2)	2.191	PEMT, PLA2G2E, PLA2G2A, PLA2G2D, PLA2G2F, PLA2G1B, PLA2G4A, PLA2G4B, PLA2G4C, PLA2G4D, PLA2G4E, PLA2G4F
PC(50:2)->LPC(32:1)	2.188	PLA2G2E, PLA2G2A, PLA2G2D, PLA2G2F, PLA2G1B, PLA2G4A, PLA2G4B, PLA2G4C, PLA2G4D, PLA2G4E, PLA2G4F
LPC(18:0)->PC(42:2)->LPC(26:1)	2.177	LPCAT1, LPCAT2, LPCAT3, LPCAT4, PLA2G2E, PLA2G2A, PLA2G2D, PLA2G2F, PLA2G1B, PLA2G4A, PLA2G4B, PLA2G4C, PLA2G4D, PLA2G4E, PLA2G4F
PA(39:6)->LPA(19:5)->PA(41:6)->PS(41:6)	2.172	PLA2G4A, PLA2G4D, PLA2G4E, PLA2G4F, AGPAT1, AGPAT2, AGPAT3, AGPAT4, AGPAT5, CDS1, PTDSS1
LPE(16:0)->PE(42:0)	2.132	MBOAT1, MBOAT2, LPCAT3, LPCAT4
PE(42:2)->PC(42:2)->LPC(26:1)	2.124	PEMT, PLA2G2E, PLA2G2A, PLA2G2D, PLA2G2F, PLA2G1B, PLA2G4A, PLA2G4B, PLA2G4C, PLA2G4D, PLA2G4E, PLA2G4F
PA(39:6)->LPA(19:5)->PA(43:7)	2.088	PLA2G4A, PLA2G4D, PLA2G4E, PLA2G4F, AGPAT1, AGPAT2, AGPAT3, AGPAT4, AGPAT5
PC(49:3)->LPC(31:3)	2.08	PLA2G2E, PLA2G2A, PLA2G2D, PLA2G2F, PLA2G1B, PLA2G4A, PLA2G4B, PLA2G4C, PLA2G4D, PLA2G4E, PLA2G4F
LPE(16:1)->PE(38:2)->PS(38:2)->LPS(18:1)->PS(38:1)	2.053	MBOAT1, MBOAT2, LPCAT3, LPCAT4, PTDSS2, PLA2G2E, PLA2G2A, PLA2G2F, MBOAT1, LPCAT3, LPCAT4
LPE(18:1)->PE(42:3)->LPE(24:1)	2.044	MBOAT1, MBOAT2, LPCAT3, LPCAT4, PLA2G4C
LPE(16:1)->PE(38:2)->PS(38:2)->LPS(18:1)->PS(35:2)->PE(35:2)->PC(35:2)->PA(35:2)	2.041	MBOAT1, MBOAT2, LPCAT3, LPCAT4, PTDSS2, PLA2G2E, PLA2G2A, PLA2G2F, MBOAT1, LPCAT3, LPCAT4, PISD, PEMT, PLD1, PLD2

PC(34:1)->PS(34:1)	2.036	PTDSS1
LPE(20:3)->PE(44:5)	2.035	MBOAT1, MBOAT2, LPCAT3, LPCAT4
LPA(20:2)->PA(40:7)	2.032	AGPAT1, AGPAT2, AGPAT3, AGPAT4, AGPAT5
LPE(16:1)->PE(38:2)->PS(38:2)->LPS(18:1)->PS(38:4)->PE(38:4)	1.986	MBOAT1, MBOAT2, LPCAT3, LPCAT4, PTDSS2, PLA2G2E, PLA2G2A, PLA2G2F, MBOAT1, LPCAT3, LPCAT4, PISD
LPE(16:0)->PE(35:2)->PC(35:2)->PA(35:2)	1.977	MBOAT1, MBOAT2, LPCAT3, LPCAT4, PEMT, PLD1, PLD2
LPA(24:3)->PA(43:5)	1.96	AGPAT1, AGPAT2, AGPAT3, AGPAT4, AGPAT5
O-LPC(20:0)->O-PC(40:3)	1.936	LPCAT1
LPE(17:0)->PE(37:2)->PS(37:2)	1.935	MBOAT1, MBOAT2, LPCAT3, LPCAT4, PTDSS2
PA(32:0)->PS(32:0)	1.93	CDS1, PTDSS1
LPE(16:1)->PE(38:2)->PS(38:2)->LPS(18:1)->PS(36:1)	1.927	MBOAT1, MBOAT2, LPCAT3, LPCAT4, PTDSS2, PLA2G2E, PLA2G2A, PLA2G2F, MBOAT1, LPCAT3, LPCAT4
LPE(16:0)->PE(40:1)->PS(40:1)	1.918	MBOAT1, MBOAT2, LPCAT3, LPCAT4, PTDSS2
LPE(16:1)->PE(38:2)->PS(38:2)->LPS(18:1)->PS(36:2)	1.917	MBOAT1, MBOAT2, LPCAT3, LPCAT4, PTDSS2, PLA2G2E, PLA2G2A, PLA2G2F, MBOAT1, LPCAT3, LPCAT4
LPE(16:0)->PE(38:1)->PS(38:1)	1.916	MBOAT1, MBOAT2, LPCAT3, LPCAT4, PTDSS2
PC(48:0)->PA(48:0)	1.913	PLD1, PLD2
LPE(16:0)->PE(40:2)->PS(40:2)	1.91	MBOAT1, MBOAT2, LPCAT3, LPCAT4, PTDSS2
LPE(16:0)->PE(35:2)->PS(35:2)	1.89	MBOAT1, MBOAT2, LPCAT3, LPCAT4, PTDSS2
LPE(32:1)->PE(52:3)	1.89	MBOAT1, MBOAT2, LPCAT3, LPCAT4
PC(44:0)->PA(44:0)->PI(44:0)	1.886	PLD1, PLD2, CDS1, CDS2, CDIPT
LPI(12:3)->PI(36:5)	1.886	MBOAT7
PC(26:0)->PA(26:0)	1.881	PLD1, PLD2
LPE(16:0)->PE(35:1)->PS(35:1)	1.878	MBOAT1, MBOAT2, LPCAT3, LPCAT4, PTDSS2
LPE(16:1)->PE(38:2)->PS(38:2)->LPS(18:1)->PS(35:1)->PE(35:1)	1.877	MBOAT1, MBOAT2, LPCAT3, LPCAT4, PTDSS2, PLA2G2E, PLA2G2A, PLA2G2F, MBOAT1, LPCAT3, LPCAT4, PISD
LPG(16:0)->PG(36:4)	1.873	LPGAT1, CRLS1
O-LPC(20:0)->O-PC(40:5)	1.871	LPCAT1
LPE(18:2)->PE(44:2)	1.86	MBOAT1, MBOAT2, LPCAT3, LPCAT4
PE(34:2)->PC(34:2)	1.854	PEMT
O-LPC(15:1)->O-PC(39:3)	1.852	LPCAT1
PC(37:2)->PA(37:2)	1.849	PLD1, PLD2
PA(30:0)->PS(30:0)	1.847	CDS1, PTDSS1

LPE(16:0)->PE(36:4)->PC(36:4)	1.831	MBOAT1, MBOAT2, LPCAT3, LPCAT4, PEMT
LPG(24:6)->PG(44:9)	1.818	LPGAT1, CRLS1
PA(32:0)->PG(32:0)	1.81	CDS1, CDS2, PTPMT1
LPE(16:0)->PE(34:0)	1.807	MBOAT1, MBOAT2, LPCAT3, LPCAT4
LPA(19:5)->PA(45:5)	1.803	AGPAT1, AGPAT2, AGPAT3, AGPAT4, AGPAT5
O-LPC(32:4)->O-PC(52:9)	1.799	LPCAT1
PE(54:5)->LPE(38:5)->PE(58:9)	1.788	PLA2G4C, MBOAT1, MBOAT2, LPCAT3, LPCAT4
PE(46:1)->PC(46:1)->LPC(30:1)->LPA(30:1)	1.78	PEMT, PLA2G2E, PLA2G2A, PLA2G2D, PLA2G2F, PLA2G1B, PLA2G4A, PLA2G4B, PLA2G4C, PLA2G4D, PLA2G4E, PLA2G4F, ENPP2
LPC(18:0)->PC(42:2)->LPC(18:1)->PC(42:3)	1.778	LPCAT1, LPCAT2, LPCAT3, LPCAT4, PLA2G2E, PLA2G2A, PLA2G2D, PLA2G2F, PLA2G1B, PLA2G4A, PLA2G4B, PLA2G4C, PLA2G4D, PLA2G4E, PLA2G4F, LPCAT1, LPCAT2, LPCAT3, LPCAT4
LPE(16:0)->PE(40:2)->PC(40:2)	1.776	MBOAT1, MBOAT2, LPCAT3, LPCAT4, PEMT
LPE(16:0)->PE(36:5)	1.775	MBOAT1, MBOAT2, LPCAT3, LPCAT4
PC(40:0)->PS(40:0)->PE(40:0)	1.77	PTDSS1, PISD
PC(42:5)->LPC(20:4)	1.763	PLA2G2E, PLA2G2A, PLA2G2D, PLA2G2F, PLA2G1B, PLA2G4A, PLA2G4B, PLA2G4C, PLA2G4D, PLA2G4E, PLA2G4F
PA(42:4)->PG(42:4)	1.758	CDS1, CDS2, PTPMT1
PA(32:0)->PI(32:0)	1.754	CDS1, CDS2, CDIPT
LPA(17:0)->PA(37:2)	1.751	AGPAT1, AGPAT2, AGPAT3, AGPAT4, AGPAT5
PC(36:1)->PS(36:1)	1.745	PTDSS1
LPE(18:1)->PE(42:3)->PC(42:3)	1.745	MBOAT1, MBOAT2, LPCAT3, LPCAT4, PEMT
LPE(16:1)->PE(38:2)->PS(38:2)->LPS(18:1)->PS(38:3)->PE(38:3)	1.744	MBOAT1, MBOAT2, LPCAT3, LPCAT4, PTDSS2, PLA2G2E, PLA2G2A, PLA2G2F, MBOAT1, LPCAT3, LPCAT4, PISD
LPE(20:0)->PE(40:0)	1.741	MBOAT1, MBOAT2, LPCAT3, LPCAT4
LPC(26:0)->LPA(26:0)	1.74	ENPP2
O-LPC(18:1)->O-PC(42:3)	1.739	LPCAT1
PE(42:2)->PC(42:2)->LPC(18:1)->PC(42:3)	1.734	PEMT, PLA2G2E, PLA2G2A, PLA2G2D, PLA2G2F, PLA2G1B, PLA2G4A, PLA2G4B, PLA2G4C, PLA2G4D, PLA2G4E, PLA2G4F, LPCAT1, LPCAT2, LPCAT3, LPCAT4
LPE(18:0)->PE(38:4)->PS(38:4)	1.724	MBOAT1, MBOAT2, LPCAT3, LPCAT4, PTDSS2
LPC(18:0)->PC(42:2)->LPC(22:1)->PC(42:6)	1.716	LPCAT1, LPCAT2, LPCAT3, LPCAT4, PLA2G2E, PLA2G2A, PLA2G2D, PLA2G2F, PLA2G1B, PLA2G4A, PLA2G4B, PLA2G4C, PLA2G4D, PLA2G4E, PLA2G4F, LPCAT1, LPCAT2, LPCAT3,

		LPCAT4
O-LPC(18:0)->O-PC(42:2)	1.714	LPCAT1
LPE(16:1)->PE(38:2)->PS(38:2)->LPS(18:1)->PS(34:1)	1.71	MBOAT1, MBOAT2, LPCAT3, LPCAT4, PTDSS2, PLA2G2E, PLA2G2A, PLA2G2F, MBOAT1, LPCAT3, LPCAT4
O-LPC(18:0)->O-PC(38:2)	1.702	LPCAT1
PA(52:4)->LPA(32:2)	1.701	PLA2G4A, PLA2G4D, PLA2G4E, PLA2G4F
LPE(16:1)->PE(38:2)->PS(38:2)->LPS(18:1)->PS(37:2)->PE(37:2)->PC(37:2)->PA(37:2)->PG(37:2)	1.701	MBOAT1, MBOAT2, LPCAT3, LPCAT4, PTDSS2, PLA2G2E, PLA2G2A, PLA2G2F, MBOAT1, LPCAT3, LPCAT4, PISD, PEMT, PLD1, PLD2, CDS1, CDS2, PTPMT1
PE(30:1)->PC(30:1)	1.698	PEMT
LPA(28:3)->PA(45:4)	1.694	AGPAT1, AGPAT2, AGPAT3, AGPAT4, AGPAT5
LPC(17:0)->PC(37:1)	1.692	LPCAT1, LPCAT2, LPCAT3, LPCAT4
LPA(24:3)->PA(43:4)	1.677	AGPAT1, AGPAT2, AGPAT3, AGPAT4, AGPAT5
O-LPC(18:0)->O-PC(37:1)	1.677	LPCAT1
PE(42:2)->PC(42:2)->LPC(22:1)->PC(42:6)	1.673	PEMT, PLA2G2E, PLA2G2A, PLA2G2D, PLA2G2F, PLA2G1B, PLA2G4A, PLA2G4B, PLA2G4C, PLA2G4D, PLA2G4E, PLA2G4F, LPCAT1, LPCAT2, LPCAT3, LPCAT4
LPS(22:1)->PS(42:1)	1.664	MBOAT1, LPCAT3, LPCAT4
LPC(20:0)->PC(40:5)->PS(40:5)->PE(40:5)	1.653	LPCAT1, LPCAT2, LPCAT3, LPCAT4, PTDSS1, PISD
O-LPC(18:0)->O-PC(38:3)	1.653	LPCAT1
LPG(16:0)->PG(36:2)	1.645	LPGAT1, CRLS1

Supplemental Table 1. BioPAN analysis of Glycerophospholipids. BioPAN analysis revealed activated and suppressed reactions in LPS treated microglia at the lipid species level.

Glycerolipids		
Activated Reactions	**Z-score**	**Predicted genes**
DG(54:9)->TG(86:13)	4.537	DGAT2
TG(46:0)->DG(28:0)->TG(48:1)	3.763	PNPLA4, PNPLA5, DGAT2
DG(28:0)->TG(48:1)	3.677	DGAT2
TG(82:5)->DG(58:4)	3.59	PNPLA4, PNPLA5
MG(14:0)->DG(30:0)->TG(54:2)	3.582	MGAT, DGAT2
MG(16:0)->DG(40:1)	3.355	MGAT
MG(14:0)->DG(32:0)	3.311	MGAT

DG(51:3)->TG(75:5)->DG(55:4)	3.214	DGAT2, PNPLA4, PNPLA5
MG(14:0)->DG(30:0)->TG(50:3)	3.207	MGAT, DGAT2
MG(16:0)->DG(36:0)	3.132	MGAT
MG(14:0)->DG(34:4)	3.124	MGAT
TG(77:6)->DG(57:6)	3.051	PNPLA4, PNPLA5
MG(18:1)->DG(38:3)	3.043	MGAT
MG(22:1)->DG(42:4)	3.025	MGAT
MG(34:2)->DG(58:4)	2.965	MGAT
DG(50:0)->MG(34:0)	2.956	PNPLA2, PNPLA3
DG(34:0)->TG(49:0)	2.925	DGAT2
MG(14:0)->DG(40:0)	2.903	MGAT
DG(37:1)->TG(57:1)	2.9	DGAT2
DG(34:3)->TG(56:4)	2.88	DGAT2
MG(22:1)->DG(46:3)	2.868	MGAT
DG(51:3)->TG(75:5)->DG(57:5)	2.844	DGAT2, PNPLA4, PNPLA5
MG(32:1)->DG(58:1)	2.826	MGAT
MG(14:0)->DG(30:0)->TG(49:1)->DG(33:1)->TG(57:2)	2.805	MGAT, DGAT2, PNPLA4, PNPLA5, DGAT2
DG(52:1)->TG(76:2)	2.791	DGAT2
MG(21:1)->DG(45:3)	2.776	MGAT
MG(22:1)->DG(46:2)	2.776	MGAT
TG(48:4)->DG(28:1)	2.764	PNPLA4, PNPLA5
MG(14:0)->DG(30:0)->TG(49:1)->DG(33:1)->TG(51:1)	2.711	MGAT, DGAT2, PNPLA4, PNPLA5, DGAT2
DG(51:3)->TG(75:5)->DG(55:5)	2.71	DGAT2, PNPLA4, PNPLA5
MG(14:0)->DG(30:0)->TG(50:2)->DG(34:2)->TG(60:2)	2.71	MGAT, DGAT2, PNPLA4, PNPLA5, DGAT2
MG(14:0)->DG(30:0)->TG(50:2)->DG(34:2)->TG(56:3)->DG(36:0)	2.701	MGAT, DGAT2, PNPLA4, PNPLA5, DGAT2, PNPLA4, PNPLA5
MG(14:0)->DG(30:0)->TG(50:2)->DG(26:1)->TG(56:6)	2.698	MGAT, DGAT2, PNPLA4, PNPLA5, DGAT2
MG(14:0)->DG(30:0)->TG(49:2)	2.673	MGAT, DGAT2
MG(14:0)->DG(30:0)->TG(54:1)	2.652	MGAT, DGAT2
MG(14:0)->DG(30:0)->TG(49:1)->DG(33:1)->TG(59:1)	2.627	MGAT, DGAT2, PNPLA4, PNPLA5, DGAT2
MG(22:1)->DG(42:6)->TG(62:11)	2.623	MGAT, DGAT2
MG(25:2)->DG(57:6)	2.58	MGAT

MG(14:0)->DG(30:0)->TG(50:2)->DG(32:1)->TG(58:1)	2.574	MGAT, DGAT2, PNPLA4, PNPLA5, DGAT2
MG(22:1)->DG(54:5)	2.538	MGAT
DG(51:3)->TG(75:5)->DG(59:5)	2.526	DGAT2, PNPLA4, PNPLA5
MG(30:0)->DG(50:4)	2.521	MGAT
DG(51:3)->TG(75:5)->DG(51:4)	2.507	DGAT2, PNPLA4, PNPLA5
MG(22:1)->DG(48:1)	2.504	MGAT
MG(14:0)->DG(32:2)	2.5	MGAT
MG(14:0)->DG(30:0)->TG(50:2)->DG(34:1)->TG(56:2)	2.469	MGAT, DGAT2, PNPLA4, PNPLA5, DGAT2
DG(26:1)->TG(56:6)	2.446	DGAT2
MG(14:0)->DG(30:0)->TG(50:2)->DG(34:1)->TG(58:2)	2.445	MGAT, DGAT2, PNPLA4, PNPLA5, DGAT2
MG(31:0)->DG(51:4)	2.442	MGAT
MG(16:0)->DG(35:1)	2.399	MGAT
TG(82:5)->DG(60:4)	2.397	PNPLA4, PNPLA5
MG(18:1)->DG(50:5)	2.382	MGAT
TG(75:5)->DG(57:4)	2.375	PNPLA4, PNPLA5
DG(37:1)->TG(59:2)	2.356	DGAT2
MG(16:0)->DG(33:0)	2.352	MGAT
MG(32:0)->DG(52:4)	2.339	MGAT
TG(75:5)->DG(55:4)	2.334	PNPLA4, PNPLA5
MG(16:0)->DG(36:3)	2.302	MGAT
MG(20:1)->DG(40:5)	2.292	MGAT
MG(14:0)->DG(30:0)->TG(49:1)->DG(33:1)->TG(53:3)	2.284	MGAT, DGAT2, PNPLA4, PNPLA5, DGAT2
MG(30:6)->DG(62:10)	2.275	MGAT
TG(77:6)->DG(59:6)	2.264	PNPLA4, PNPLA5
MG(14:0)->DG(30:0)->TG(50:2)->DG(32:1)->TG(52:6)	2.264	MGAT, DGAT2, PNPLA4, PNPLA5, DGAT2
MG(18:1)->DG(38:5)->TG(58:8)	2.262	MGAT, DGAT2
DG(51:3)->TG(75:5)->DG(53:4)	2.239	DGAT2, PNPLA4, PNPLA5
MG(16:1)->DG(42:1)	2.227	MGAT
MG(34:2)->DG(60:2)	2.211	MGAT
MG(20:1)->DG(40:6)	2.206	MGAT
MG(21:1)->DG(45:2)	2.201	MGAT
DG(30:0)->TG(49:1)	2.199	DGAT2

MG(16:0)->DG(36:4)->TG(56:7)->DG(38:5)->TG(58:8)	2.177	MGAT, DGAT2, PNPLA4, PNPLA5, DGAT2
DG(30:0)->TG(50:2)	2.168	DGAT2
MG(21:1)->DG(53:5)	2.166	MGAT
MG(16:0)->DG(36:2)	2.16	MGAT
MG(24:2)->DG(56:6)	2.137	MGAT
MG(31:1)->DG(64:7)	2.134	MGAT
MG(14:0)->DG(44:5)	2.132	MGAT
MG(14:0)->DG(36:1)	2.107	MGAT
MG(14:0)->DG(34:2)	2.103	MGAT
MG(14:0)->DG(30:0)->TG(49:1)->DG(33:1)->TG(52:3)	2.099	MGAT, DGAT2, PNPLA4, PNPLA5, DGAT2
DG(30:0)->TG(54:2)	2.08	DGAT2
MG(16:0)->DG(35:2)	2.064	MGAT
TG(72:2)->DG(56:1)	2.062	PNPLA4, PNPLA5
MG(14:0)->DG(30:0)->TG(50:2)->DG(32:2)	2.06	MGAT, DGAT2, PNPLA4, PNPLA5
DG(33:1)->TG(57:2)	2.057	DGAT2
DG(24:0)->TG(42:0)	2.057	DGAT2
DG(32:1)->TG(58:1)	2.053	DGAT2
MG(16:0)->DG(36:4)->TG(56:7)->DG(36:3)	2.031	MGAT, DGAT2, PNPLA4, PNPLA5
MG(16:0)->DG(36:4)->TG(56:7)->DG(40:7)	2.021	MGAT, DGAT2, PNPLA4, PNPLA5
DG(34:1)->TG(56:2)	2.016	DGAT2
DG(24:0)->TG(44:2)	1.995	DGAT2
MG(16:0)->DG(40:2)->TG(62:3)->DG(46:3)	1.981	MGAT, DGAT2, PNPLA4, PNPLA5
MG(32:1)->DG(62:6)	1.979	MGAT
TG(77:6)->DG(53:5)	1.972	PNPLA4, PNPLA5
DG(34:1)->TG(58:2)	1.967	DGAT2
MG(18:1)->DG(44:1)	1.953	MGAT
MG(20:1)->DG(52:5)	1.952	MGAT
MG(31:1)->DG(47:2)	1.939	MGAT
MG(21:1)->DG(54:7)	1.934	MGAT
MG(14:0)->DG(30:0)->TG(50:2)->DG(34:2)->TG(54:3)	1.923	MGAT, DGAT2, PNPLA4, PNPLA5, DGAT2
DG(47:1)->TG(79:5)	1.908	DGAT2
DG(34:3)->TG(52:5)	1.904	DGAT2
TG(65:6)->DG(45:3)	1.87	PNPLA4, PNPLA5

DG(33:1)->TG(51:1)	1.868	DGAT2
MG(16:0)->DG(36:4)->TG(56:7)->DG(40:6)	1.861	MGAT, DGAT2, PNPLA4, PNPLA5
MG(20:4)->DG(40:7)->TG(60:11)->DG(42:9)	1.86	MGAT, DGAT2, PNPLA4, PNPLA5
MG(34:3)->DG(58:5)	1.848	MGAT
DG(32:7)->TG(47:8)	1.83	DGAT2
MG(20:1)->DG(40:4)	1.827	MGAT
DG(32:7)->TG(58:7)	1.818	DGAT2
TG(75:5)->DG(57:5)	1.811	PNPLA4, PNPLA5
MG(16:0)->DG(36:4)->TG(56:7)->DG(38:6)	1.81	MGAT, DGAT2, PNPLA4, PNPLA5
MG(18:1)->DG(38:4)	1.796	MGAT
DG(24:0)->TG(42:1)	1.791	DGAT2
MG(14:0)->DG(33:1)->TG(53:1)	1.764	MGAT, DGAT2
TG(74:1)->DG(58:1)	1.751	PNPLA4, PNPLA5
TG(46:0)->DG(26:0)->TG(45:2)	1.739	PNPLA4, PNPLA5, DGAT2
DG(36:4)->TG(56:7)	1.713	DGAT2
MG(14:0)->DG(30:0)->TG(49:1)->DG(33:0)	1.708	MGAT, DGAT2, PNPLA4, PNPLA5
DG(33:1)->TG(59:1)	1.7	DGAT2
DG(51:3)->TG(75:5)->DG(57:4)->TG(90:10)	1.68	DGAT2, PNPLA4, PNPLA5, DGAT2
MG(18:1)->DG(37:2)	1.674	MGAT
DG(24:0)->TG(40:0)	1.663	DGAT2
MG(14:0)->DG(34:1)	1.662	MGAT
MG(20:1)->DG(46:1)	1.661	MGAT
TG(64:3)->DG(48:2)	1.658	PNPLA4, PNPLA5
MG(14:0)->DG(30:1)->TG(56:1)	1.658	MGAT, DGAT2
MG(14:0)->DG(30:1)->TG(60:6)	1.646	MGAT, DGAT2
Suppressed Reactions	**Z-score**	**Predicted genes**
DG(30:0)->TG(47:0)	3.288	DGAT2
TG(62:2)->DG(46:2)	3.119	PNPLA4, PNPLA5
TG(58:1)->DG(42:1)	3.061	PNPLA4, PNPLA5
TG(56:7)->DG(36:4)->MG(20:4)->DG(35:4)	3.024	PNPLA4, PNPLA5, PNPLA2, PNPLA3, MGAT
TG(79:5)->DG(59:2)	2.929	PNPLA4, PNPLA5
TG(56:7)->DG(36:2)	2.858	PNPLA4, PNPLA5
DG(54:5)->TG(87:11)	2.723	DGAT2
TG(72:2)->DG(56:2)	2.597	PNPLA4, PNPLA5

TG(58:1)->DG(40:0)	2.582	PNPLA4, PNPLA5
MG(34:0)->DG(54:0)	2.577	MGAT
DG(28:0)->TG(48:0)	2.451	DGAT2
DG(40:2)->MG(22:1)	2.437	PNPLA2, PNPLA3
DG(54:2)->MG(34:1)->DG(58:3)	2.436	PNPLA2, PNPLA3, MGAT
TG(54:4)->DG(34:3)	2.431	PNPLA4, PNPLA5
TG(56:7)->DG(38:6)	2.404	PNPLA4, PNPLA5
TG(56:7)->DG(36:4)->MG(20:4)->DG(42:5)	2.375	PNPLA4, PNPLA5, PNPLA2, PNPLA3, MGAT
DG(34:4)->TG(49:5)	2.372	DGAT2
MG(30:0)->DG(52:1)->TG(78:1)	2.354	MGAT, DGAT2
TG(56:7)->DG(40:6)	2.315	PNPLA4, PNPLA5
DG(54:7)->MG(30:6)	2.286	PNPLA2, PNPLA3
DG(36:4)->MG(20:4)->DG(35:4)	2.276	PNPLA2, PNPLA3, MGAT
TG(86:13)->DG(66:8)	2.273	PNPLA4, PNPLA5
TG(60:1)->DG(44:1)	2.263	PNPLA4, PNPLA5
DG(34:2)->MG(16:1)->DG(35:3)	2.258	PNPLA2, PNPLA3, MGAT
TG(58:5)->DG(42:4)	2.25	PNPLA4, PNPLA5
TG(50:2)->DG(34:1)	2.232	PNPLA4, PNPLA5
TG(56:7)->DG(38:5)	2.211	PNPLA4, PNPLA5
TG(50:2)->DG(26:1)	2.205	PNPLA4, PNPLA5
MG(32:0)->DG(56:2)	2.202	MGAT
DG(34:2)->MG(16:0)	2.137	PNPLA2, PNPLA3
TG(53:3)->DG(37:2)	2.125	PNPLA4, PNPLA5
TG(58:7)->DG(42:6)	2.124	PNPLA4, PNPLA5
TG(60:2)->DG(44:2)	2.108	PNPLA4, PNPLA5
TG(58:5)->DG(42:5)	2.107	PNPLA4, PNPLA5
TG(54:4)->DG(34:0)	2.062	PNPLA4, PNPLA5
TG(50:2)->DG(32:1)	2.06	PNPLA4, PNPLA5
TG(53:3)->DG(33:3)	2.03	PNPLA4, PNPLA5
TG(56:7)->DG(36:3)	2.022	PNPLA4, PNPLA5
TG(57:2)->DG(41:2)->MG(25:2)->DG(47:3)	2.014	PNPLA4, PNPLA5, PNPLA2, PNPLA3, MGAT
DG(51:1)->MG(33:0)	2.006	PNPLA2, PNPLA3
TG(58:5)->DG(40:5)	1.999	PNPLA4, PNPLA5
TG(76:2)->DG(58:2)	1.997	PNPLA4, PNPLA5
TG(72:2)->DG(52:1)->TG(78:1)	1.975	PNPLA4, PNPLA5, DGAT2

TG(57:1)->DG(41:1)	1.965	PNPLA4, PNPLA5
TG(50:2)->DG(32:0)	1.964	PNPLA4, PNPLA5
DG(30:0)->TG(50:5)	1.939	DGAT2
TG(76:2)->DG(60:2)	1.912	PNPLA4, PNPLA5
TG(60:3)->DG(44:3)	1.894	PNPLA4, PNPLA5
TG(49:1)->DG(33:0)->TG(53:0)	1.889	PNPLA4, PNPLA5, DGAT2
TG(58:3)->DG(42:3)	1.886	PNPLA4, PNPLA5
DG(28:0)->TG(48:4)->DG(30:2)	1.872	DGAT2, PNPLA4, PNPLA5
DG(30:0)->MG(14:0)	1.869	PNPLA2, PNPLA3
DG(56:5)->TG(82:5)	1.865	DGAT2
DG(28:0)->TG(48:5)	1.834	DGAT2
DG(34:2)->MG(18:1)->DG(38:6)	1.833	PNPLA2, PNPLA3, MGAT
DG(34:2)->MG(18:1)->DG(42:3)	1.829	PNPLA2, PNPLA3, MGAT
TG(58:7)->DG(42:7)	1.805	PNPLA4, PNPLA5
TG(62:2)->DG(46:1)	1.803	PNPLA4, PNPLA5
MG(30:0)->DG(50:0)	1.79	MGAT
TG(58:3)->DG(42:2)	1.764	PNPLA4, PNPLA5
TG(58:5)->DG(40:4)	1.742	PNPLA4, PNPLA5
DG(48:1)->MG(32:1)	1.698	PNPLA2, PNPLA3
TG(56:7)->DG(40:7)->TG(60:11)	1.686	PNPLA4, PNPLA5, DGAT2
DG(57:4)->TG(90:10)	1.676	DGAT2
TG(40:1)->DG(24:0)	1.664	PNPLA4, PNPLA5

Supplemental Table 2. BioPAN analysis of Glycerolipids. BioPAN analysis revealed activated and suppressed reactions in LPS treated microglia at the lipid species level.